Journal of Biomedical Optics

BiomedicalOptics.SPIEDigitalLibrary.org

Measuring protein dynamics in live cells: protocols and practical considerations for fluorescence fluctuation microscopy

Robert T. Youker
Haibing Teng

SPIE.

Journal of Biomedical Optics 19(9), 090801 (September 2014)

TUTORIAL

Measuring protein dynamics in live cells: protocols and practical considerations for fluorescence fluctuation microscopy

Robert T. Youker[a,b,*,†] **and Haibing Teng**[c,‡]
[a]University of Pittsburgh School of Medicine, Renal-Electrolyte Division, Pittsburgh, Pennsylvania 15261, United States
[b]Western Carolina University, Department of Biology, Cullowhee, North Carolina 28723, United States
[c]Carnegie Mellon University, Molecular Biosensor and Imaging Center (MBIC), Pittsburgh, Pennsylvania 15213, United States

Abstract. Quantitative analysis of protein complex stoichiometries and mobilities are critical for elucidating the mechanisms that regulate cellular pathways. Fluorescence fluctuation spectroscopy (FFS) techniques can measure protein dynamics, such as diffusion coefficients and formation of complexes, with extraordinary precision and sensitivity. Complete calibration and characterization of the microscope instrument is necessary in order to avoid artifacts during data acquisition and to capitalize on the full capabilities of FFS techniques. We provide an overview of the theory behind FFS techniques, discuss calibration procedures, provide protocols, and give practical considerations for performing FFS experiments. One important parameter recovered from FFS measurements is the relative molecular brightness that can correlate with oligomerization. Three methods for measuring molecular brightness (fluorescence correlation spectroscopy, photon-counting histogram, and number and brightness analysis) recover similar values when measuring samples under ideal conditions *in vitro*. However, examples are given illustrating that these different methods used for calculating molecular brightness of fluorescent molecules in cells are not always equivalent. Methods relying on spot measurements are more prone to bleaching and movement artifacts that can lead to underestimation of brightness values. We advocate for the use of multiple FFS techniques to study molecular brightnesses to overcome and compliment limitations of individual techniques. [DOI: 10.1117/1.JBO.19.9.090801]

Keywords: molecular brightness; fluorescence fluctuation spectroscopy; tutorial; biophysical techniques; Paxillin; protein dynamics.

Paper 140104TR received Feb. 20, 2014; revised manuscript received Aug. 12, 2014; accepted for publication Jul. 31, 2014; published online Sep. 26, 2014.

1 Introduction

In the past 15 to 20 years, there has been an explosion in the advancement of imaging instrumentation and analytical tools to measure molecular dynamics in live cells. Diverse processes such as chemical kinetics, molecular diffusion, protein transport, protein oligomerization, molecular interactions, and stoichiometries can now be followed with single molecule sensitivity and at microsecond timescales in biological systems.[1–18] These microscopy-based techniques that make up this burgeoning field at the interface of biology and physics are collectively called fluorescence fluctuation spectroscopy (FFS) techniques (for review, see Refs. 19–21). At the heart of FFS techniques lies the ability to extract molecular dynamic information, such as diffusion and size, through analysis of the fluctuations that occur in the fluorescent signal emitted from the molecule of interest (Fig. 1). In fluorescence correlation spectroscopy (FCS), the time-dependent variation in the fluorescent signal is analyzed using an autocorrelation function to determine diffusion rates and concentrations of molecular species.[22,23] However, the size/hydrodynamic radius of a molecular species can be difficult to measure by FCS because the diffusion rate of a molecule is proportional to the cube root of its volume. This means that the size must increase about eightfold to detect a twofold increase in the diffusion rate.[24] To circumvent this limitation, the complementary approach of photon-counting histogram (PCH) analysis, using the same dataset collected from FCS, was developed to extract the average number of fluorophores in the diffusing species.[25,26] If the diffusing species are homogenous and do not contain unlabeled molecules, then the oligomerization state can be inferred by comparing the molecular brightness of the unknown species to a control (monomer or dimer). In PCH analysis, the photons of the fluorescent signal are counted to plot a histogram and the ratio of the signal fluctuations (variance) to average intensity is calculated to give the molecular brightness defined as counts per second per molecule (CPSM, Ref. 25). Therefore, the average fluorescent intensity of a 0.5-nM solution of a dimer (two fluorescent dyes) would have the same average intensity as 1 nM of a monomer (one fluorescent dye), but the molecular brightness of the dimer would be twice that of the monomer due to the larger variance. Fluorescence cross-correlation spectroscopy and dual-color PCH are FFS techniques used to measure the dynamics of two different fluorescently labeled molecules (e.g., green and red fluorophores) and are robust in detecting complex formation and dissociation events.[19,20] The imaging extensions of FCS and PCH analyses

*Address all correspondence to: Robert T. Youker, E-mail: rtyouker@wcu.edu

†Current address: Western Carolina University, Department of Biology, 111 Memorial Drive, Natural Science Building, Room 128, Cullowhee, North Carolina 28723, United States

‡Current address: Carnegie Mellon University, MBIC/Biological Sciences, 4400 Fifth Avenue, Pittsburgh, Pennsylvania 15213, United States

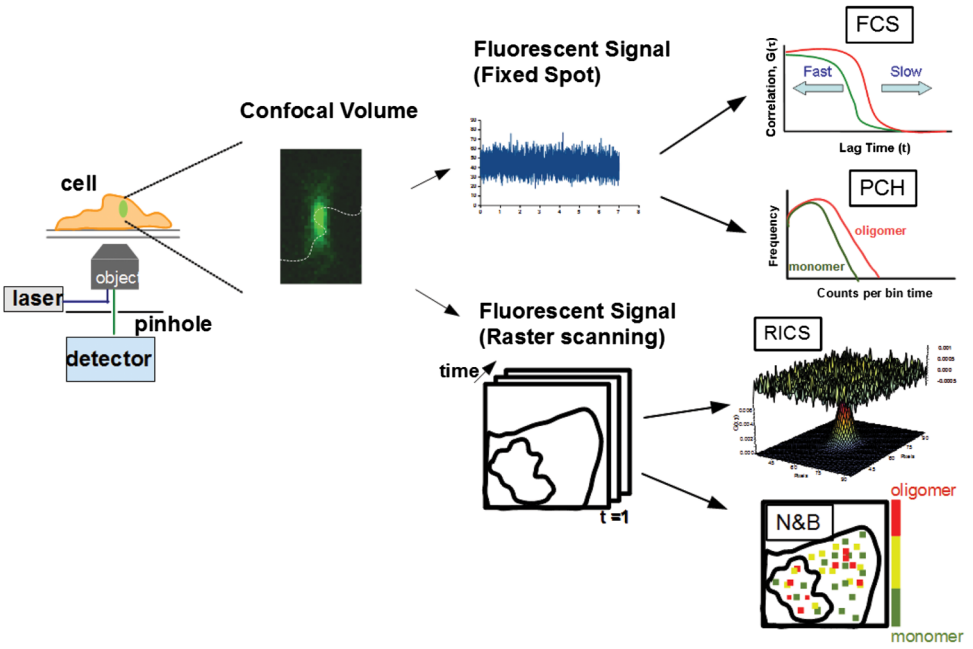

Fig. 1 Schematic illustrating four fluorescence fluctuation techniques (FFTs) used to measure protein dynamics in cells. Left: cartoon depiction of cell being imaged using a confocal microscope setup. *XZ* fluorescent image of one-photon confocal volume with dotted line superimposed to represent the random diffusion of a fluorescently labeled molecule. Middle: fluorescent signal trace from a single fixed spot in the cell, or the laser beam can be raster scanned to record frames of images in the cell. Right: autocorrelation curves [fluorescence correlation spectroscopy (FCS)] from spot measurements can be fitted to obtain diffusion rates for the fluorescent molecules. The same dataset can be used to generate a photon-counting histogram (PCH) that can be fitted to obtain a molecular brightness. Diffusion [raster image correlation spectroscopy (RICS)] and molecular brightness [number and brightness (N&B)] values can be extracted from the raster scan images on a per pixel basis to generate spatiotemporal diffusion and molecular brightness maps, respectively.

are called raster image correlation spectroscopy (RICS) and number and brightness (N&B) analysis, respectively.[21,27,28] RICS and N&B analyses allow for the spatiotemporal mapping of protein dynamics across an entire cell on microsecond to second time scales by exploiting the hidden time structure of the scanning laser beam of a confocal microscope. For example, examination of the spatial spread of the diffusion using RICS can help distinguish between simple diffusion and the binding/unbinding equilibria that can be more difficult to determine by spot measurements.

The molecular brightness can be ascertained by FCS, PCH, or N&B analysis if the data are properly acquired and normalized to control(s), thus yielding information about the stoichiometry of the diffusing specie(s). In fact, MacDonald and colleagues have shown that under optimal conditions, the brightness of AlexaFluor-488 dye is similar regardless of the techniques used.[29] Importantly, FFS techniques rely on the statistical analysis of the fluctuations in the fluorescent signal to extract dynamic information about the diffusing species; any fluctuations not due to the molecular processes under investigation, such as system instabilities, will generate artifacts that complicate interpretations of the collected data. System instabilities that can contaminate the signal include fluctuations due to stage drift, sample movement, laser power variations, illumination volume geometry artifacts, undesired photophysics of fluorophore, and photobleaching of the fluorescence.

Measurements of molecular brightness in living systems, such as eukaryotic cells, are not optimal due to a variety of diverse factors that include cellular movement, sample thickness bias, geometric constraints, and slow diffusion of molecules leading to a greater propensity for photobleaching.[29–33] Are all brightness analysis techniques equivalent when studying protein dynamics inside complex living systems under nonideal conditions? The purpose of this tutorial is twofold: (1) provide practical advice for the implementation of three widely used FFS techniques (FCS, PCH, and N&B) in measuring the molecular brightness of proteins in live cells and (2) provide two examples where these techniques are not equivalent in determining molecular brightness due to system instabilities, properties of the protein under investigation, or the mode of acquisition (spot scan versus raster scan).

2 Theory of Fluorescence Fluctuation Spectroscopy Techniques

Several excellent reviews have been written describing the theory of FFS techniques and the reader is directed to these sources for an in-depth theoretical discussion.[19–21,34–36] Summarized below are the basic principles and underlying statistical analyses used to extract molecular brightness values from fluorescence intensity measurements for FCS, PCH, and N&B methods.

2.1 *FCS Analysis*

The basis of FCS analysis is that the fluorescent intensity is varying because molecules enter and leave the illumination volume over time due to Brownian or directed diffusion. For the FCS technique to work, the concentration of the molecules

under investigation must be low, nanomolar to micromolar range, for the fluctuations not to be averaged out. This is trivial to achieve *in vitro* where the concentration of the molecules to be studied can be easily manipulated. This requirement for low concentrations of particles limited the use of FCS for biological measurements until the invention of the confocal microscope in the 1990s even though FCS has been employed since the late 1970s to study molecular dynamics *in vitro*.[10,11,22,23] Today's confocal microscopes can typically create a diffraction-limited spot (illumination volume) to ~1 fl if the pinhole is kept to ≤ 1 Airy unit (AU) (Fig. 1, left panel). The change in the fluorescent intensity (δI) at equilibrium is determined by subtracting the average intensity (brackets indicate average) from the signal intensity at a given time [Eq. (1)]:

$$\delta I(t) = I(t) - \langle I(t) \rangle. \tag{1}$$

Comparison of δI to itself at different lag times (τ) is called the autocorrelation function [$G(\tau)$], which is a measure of the similarity of the signal to itself over time [Eq. (2)]:

$$G(\tau) = \frac{\langle \delta I(t) \cdot \delta I(t+\tau) \rangle}{\langle I(t) \rangle^2}. \tag{2}$$

Plotting the autocorrelation function [$G(\tau)$] versus time creates an FCS curve with a characteristic decay for the species being investigated (Fig. 1, right panel). The time corresponding to the half maximum of the fitted autocorrelation curve is the diffusion time of the molecule. Calibration of the waist of the illumination volume is needed to determine the diffusion rate and can be calculated by several different means, such as measurement of a fluorophore with a known diffusion coefficient or imaging of diffraction-limited beads (see Sec. 3.1). The inverse of the amplitude of the FCS curve at G_o is equal to the average number of particles diffusing through the illumination volume but only if the number of fluctuations obey Poisson statistics. Therefore, the molecular brightness (ε) of the diffusing species can be calculated by dividing the average count rate ($\langle k \rangle$) by the average number of particles (N) recovered from the FCS curve fit ($\varepsilon = \langle k \rangle / N$). Concentration measurements can also be made once the N and volume have been determined, providing a robust way to measure concentration differences in cellular compartments.

The relationship between the fluctuation intensity and the average number of particles in the illumination volume has been exploited by several groups to study protein dimerization and protein ligand interactions using the inverse relationship between the particle number and amplitude of the FCS curve (G_o). In the case of dimerization, as the particle number drops to half because of complex formation, the fluctuation amplitude of the FCS curve (G_o) will double.[37–41] This relationship holds true if the total protein concentration is stable during the FCS measurement. This method of using intensity (first moment) and variance (second moment) information from FCS measurements to calculate molecular brightness is termed moment analysis. Moment analysis is successful when applied to homogenous single species samples, but interpretation of the fluctuation amplitude is very difficult when there are multiple species of varying concentrations because molecular brightness contributes nonlinearly to the fluctuation amplitude.[29,42] In addition, higher moments and a much larger dataset are required to adequately describe all species using moment analysis on FCS datasets.[29] Therefore, the exact concentrations of the different species must be known to adequately describe the amplitude and G_o, which is not always possible. For these reasons, complementary approaches to analyze fluctuation amplitudes for determination of molecular brightness and number information for multiple species were developed, such as PCH analysis.

2.2 *RICS Analysis*

In FCS analysis, only signal fluctuations at one point of illumination are measured, but in RICS analysis, fluctuations from multiple volumes are considered both near (adjacent pixels) and far (nonadjacent pixels). This allows a more complete description of the probability of finding a diffusing particle in space and time. A single spot measurement would be sufficient to describe the isotropic diffusion of a particle because its movement is uniform in space and time. In contrast, RICS is better suited for the measurement of particles with anisotropic behavior (diffusion rate varying in space and time) compared to FCS. Importantly, the pixel dwell time and pixel size must be compatible with the particle diffusion being studied in order to perform RICS measurements. If the scan speed is too fast, then the particle will appear immobile, but if the speed is too slow, then the particle will diffuse away before being detected in subsequent pixels. Pixel sizes ranging from 0.025 to 0.2 μm and pixel dwell times ranging from 2 to 100 μs will be sufficient to measure the dynamics of a wide range of molecular species. For example, a pixel size of ≤ 0.05 μm and dwell time of 25 μs are sufficient for capturing the movement of a 25 kDa protein diffusing in the cytoplasm of a cell by pixel 2-3 of the scan.[21,28] To prevent undersampling, a minimum region of interest (ROI) of 2 μm × 2 μm is recommended by Brown and colleagues based on simulations and experimental measurements of enhanced green fluorescent protein (EGFP) in solution.[43] The typical resolution of RICS is ~0.8 μm based on a 16-pixel subframe commonly used for analysis (16 pixels averaged; 0.05 μm size) and is approximately two to three fold lower than FCS.[21] Finally, cellular movement or immobile structures within cells can lead to artifacts in the correlation function and, therefore, a high-pass filter algorithm may be needed during image analysis.

2.3 *PCH Analysis*

The amplitudes of the fluorescence signal can be analyzed by binning the data and plotting frequency as a function of photon counts per bin-time, which is called a PCH histogram plot. In this way, the entire photon distribution can be considered based on the first and second moments of the signal. A PCH plot of a single molecular species can be fully characterized by defining the average number of molecules per illumination volume and the photon counts per molecule per second (i.e., molecular brightness, ε). The shape of the plot is influenced by the intensity heterogeneity of the point spread function (PSF), Poisson shot noise from the detector, and fluctuation in molecule numbers. Any fitting method must account for these variables to obtain an accurate molecular brightness. The histogram is fitted using a nonlinear least square fitting method, such as Levenberg-Marquardt or Gauss-Newton, to equation $\sigma^2 = Mp(k)[1 - p(k)]$ to obtain the variance (σ^2), where $p(k)$ is the probability of the measured photon counts in a bin and M is the total number of measurements. In the above-mentioned equation, intensity (I) and photon counts (k) are interchangeable under these circumstances, but k is used because it pertains to fitting a PCH plot. The variance and average intensity of the signal are then

inserted into Eq. (3) to calculate the molecular brightness of the molecule:

$$\langle \varepsilon \rangle = \frac{(\sigma^2 - \langle I \rangle)}{\gamma \langle I \rangle} = \sum_i f_i \varepsilon_i, \tag{3}$$

where σ^2 is the variance, I is the intensity of the signal, f represents the fractional intensity of species, and γ is the geometric shape of the PSF.[42] If there are two molecular species in the sample, for example, the resultant histogram will be convolved to reflect the contributions from both species and the histogram can be fitted to obtain additional N&B parameters to account for the extra species. Additional analytical methods that use different mathematical approaches but are functionally equivalent to PCH analysis have been described but will not be discussed here and the reader is directed to Refs. 44–46 for more information. Finally, methods have been developed that allow the determination of brightness and diffusion information by combining the advantages of FCS and PCH.[47]

2.4 *N&B Analysis*

It is cumbersome to perform FCS and PCH measurements on biological samples, such as eukaryotic cells, because only a single illumination volume in a selected location can be measured. Measuring the entire cell would take an inordinately long time, require a large number of observations per image pixel, and would be computationally slow. N&B analysis allows the extraction of average molecular brightness and numbers of particles from individual pixels of a raster scanned image using moment analysis.[27] The method was originally developed to study the aggregation state of a protein subunit during assembly/disassembly of focal adhesion complexes.[16] In N&B analysis, the average counts per integration time ($\langle k \rangle$) and variance (σ^2) at each pixel is calculated and the following two equations are used to calculate average apparent brightness [B, Eq. (4)] and apparent number of particles [N, Eq. (5)]:

$$B = \frac{\langle k \rangle}{N} = \frac{\sigma^2}{\langle k \rangle} = \varepsilon + 1, \tag{4}$$

$$N = \frac{\langle k \rangle^2}{\sigma^2}. \tag{5}$$

Variances from the fluorescent molecules (dim fast diffusing, bright slow diffusing, and immobile), autofluorescence, light scattering, and noises of the detector all contribute to the total signal variance. If these sources of variance are independent, the total variance is simply the sum of the individual variances. Fortunately, these variances do not have to be accounted for individually because only the mobile molecules/particle fluctuations vary with the square of the brightness ($\sigma_n^2 = \varepsilon^2 n$) leading to a B value >1.[27] In contrast, immobile particles do not have fluorescence fluctuations so that the variance (σ^2) in the pixel and the ratio of variance/$\langle k \rangle$ are zero and B is 1. An increase of the illumination intensity can be used to confirm that the variance originates from the particles of interest because a plot of variance as a function of intensity should have a quadratic relationship. Subtraction of 1 from B yields a true molecular brightness ε. This is necessary in order to remove the detector count statistics that contribute to the variance (for the mathematical basis, see Ref. 27). The true number of particles n can be calculated using the following equation [Eq. (6)]. Again, this is necessary to correct for the noise contributed by the detector.

$$n = \frac{\langle k \rangle^2}{\sigma^2 - \langle k \rangle}. \tag{6}$$

It is important to select an appropriate pixel dwell time that is long enough to adequately sample the fluctuations but avoids averaging out the signal fluctuations. For example, a pixel dwell time of 25 μs is reasonable if one is studying a protein diffusing inside a cell at $\sim$20 $\mu m^2/s$.

Photon-counting detectors are ideal for N&B measurements because the registered photon event correlates one-to-one with the signal generated unlike analog detector systems that record digital levels. However, analog systems can be used for N&B analysis as long as the average count rate ($\langle k \rangle$) and B values are corrected for the digital offset (d) and digital levels per photon (S), respectively [Eqs. (7) and (8), Refs. 21 and 48]:

$$\langle k \rangle = \varepsilon n + d, \qquad n = \frac{\langle N \rangle B}{B - S}, \tag{7}$$

$$\varepsilon = B - S. \tag{8}$$

Each time the voltage or gain is changed on the analog detector, the calibration must be repeated to determine the new S value. Limitations to N&B analysis are that fast-moving particles, such as fluorescent dyes, in solution sometimes cannot be measured and the observation volume is roughly three fold larger in the x-y plane compared to the volume for FCS/PCH measurements because of the raster scanning of the laser. Importantly, mixtures of multiple species with different brightnesses residing in the same pixel cannot be resolved by N&B analysis and only the weighted average brightnesses obtained.[27] In contrast, the technique is robust for identifying spatially heterogeneous clusters of particles/species in an image.[7,9,15,16,27]

2.5 *Summary of FFS Theories*

Molecular brightness determination using FCS data is well suited for homogenous single species, but this method breaks down in the face of more complex heterogeneous samples. In contrast, the PCH method for calculating molecular brightness takes the entire photon-count distribution into consideration and can be used to resolve samples containing multiple species of varying brightness. The recently developed technique of N&B analysis applies moment analysis to extract N&B information from individual pixels of a raster scanned image, making it amenable for measuring biological samples, such as cells. The molecular oligomerization measured by FFTs represents the minimum stoichiometries in systems where fluorescently labeled and unlabeled molecules coexist. Therefore, it is useful to perform experiments in the absence of unlabeled molecules when possible. Importantly, the brightness values obtained from all three measurements depend on the laser intensity employed. For example, higher laser powers will give rise to higher brightness values. The intrinsic characteristics of the detector, such as dead-time and afterpulsing, also affect the brightness values obtained. For these reasons, all measurements should be performed at the same detector and laser power settings. Routinely, relative brightness values are given instead of absolute values for comparison since different research groups have different experimental setups.

3 Calibration of Microscope for FFS Measurements

3.1 *Calibration of Detection Volume*

We recommend periodically checking the size and shape of the confocal volume (once every three months) to identify any deviations that could arise due to system damage/misalignment. Three commonly used methods to measure the shape and size of the confocal volume are (1) dilution series measurement of a dye with a known concentration, (2) measurement of a dye with a known diffusion coefficient, and (3) measurement from raster scanned images of the subresolution fluorescent bead.

The advantages of the first method for volume determination are that the calibration and experiment can be performed under similar conditions and no information about the shape of the volume is needed. This is because the effective volume (V_{eff}) can be calculated using G_{o} (correlation amplitude), Avogadro's number (Na), and the concentration of the solution (C) and without mathematical fitting of the FCS curve by using Eq. (9):

$$V_{\text{eff}} = \frac{1}{G_{\text{o}} N_{\text{a}} C}. \tag{9}$$

The second method does not require knowledge of the solution's concentration but only the known diffusion coefficient (D) for the fluorescent molecule. This method does assume the effective volume is Gaussian and the effective volume can be calculated using Eq. (10):

$$V_{\text{eff}} = \pi^{3/2} S (4 D \tau_D)^{3/2}. \tag{10}$$

Solving Eq. (10) is usually done with D fixed and the other variables (S, eccentricity/structural parameter = ratio of axial radius to lateral radius; τ_D = diffusion time) obtained from the fitted FCS curve.

Unlike the first two methods, the third method directly measures the confocal volume (V_{conf}) using subresolution fluorescent beads as a point source and V_{conf} can be converted to the V_{eff} using Eq. (11):

$$V_{\text{conf}} = \left(\frac{\pi}{2}\right)^{3/2} \cdot \omega_o^2 z_o = (1/2)^{3/2} \cdot V_{\text{eff}}. \tag{11}$$

A bead size of 100 to 170 nm is suitable for calibration and the size will not impact the calibration as long as it is smaller than the diffraction-limited spot. There is a freely available ImageJ plugin that automates the analysis of the fluorescent bead image series that we have found quite helpful.[49] All three methods yield comparable results and the bead scanning method is particularly fast when image analysis is automated using ImageJ. For a more in-depth discussion of volume calibration methods, see the PicoQuant application note.[50]

3.2 *Determination of Detector Sensitivity*

The microscope detector sensitivity and optimal laser power must be determined before the molecular brightness of the sample can be measured. Measurement of either a purified fluorescent dye or fluorescent protein to be used in the experiment is a good choice for characterizing the microscope system. Since many of our experiments involve measuring the dynamics of GFP-tagged proteins in mammalian cells, we chose to use purified EGFP to characterize our one-photon Zeiss LSM 510 META ConfoCor 3 microscope system. The following calibration experiments are applicable to characterize all microscope systems equipped to perform FFT measurements. First, we measured different concentrations of purified EGFP in solution using a constant low laser power setting [0.45 μW at the sample level, 488 nm argon laser, Fig. 2(a)]. The molecular brightness was determined either from fitted FCS data by

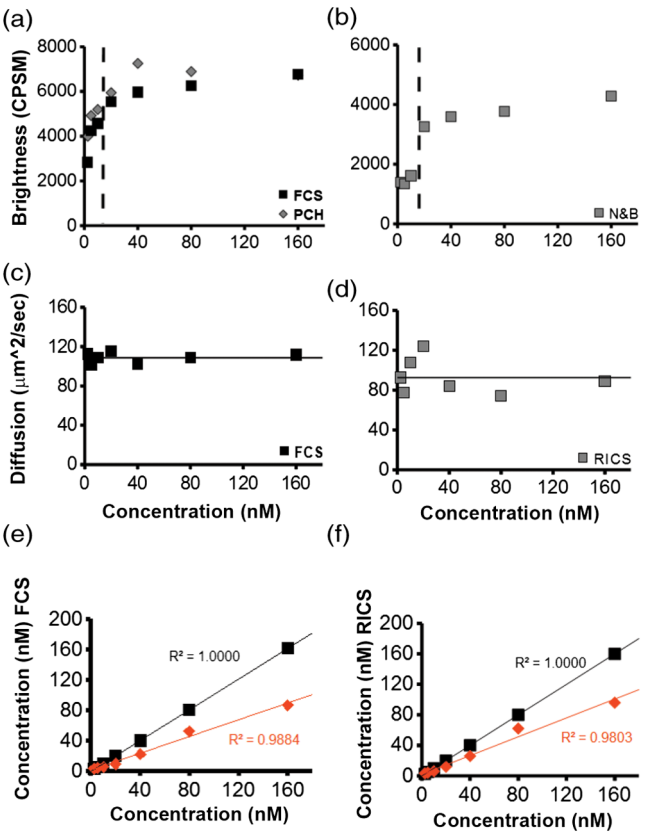

Fig. 2 Characterization of microscope system detector sensitivity. The concentrations of the enhanced green fluorescent protein (EGFP) solution were varied from 2.5 to 160 nM. The laser power was attenuated to 0.45 μW, at the sample level, of a 30-mW argon laser. (a) Plot of molecular brightness expressed as counts per second per molecule (CPSM) as a function of the EGFP concentration measured *in vitro* using either FCS (black squares) or PCH (gray diamonds) methods. (b) Plot of molecular brightness (CPSM) as a function of the EGFP concentrations based on N&B analysis. (c) and (d) Recovered diffusion coefficients as a function of the EGFP concentrations using FCS or RICS analysis, respectively. (e) and (f) Plot of EGFP concentration measured by spectrophotometer absorbance as a function of concentration measured by FCS or RICS analysis, respectively. Concentration calculated using effective (black squares) or confocal volume (orange diamonds) from 2.5, 5, 10, 20, 40, 80, and 160 nM EGFP solutions. Effective volume calculated using Eq. (9) and confocal volume determined from images of subresolution fluorescent beads using the equation $V_{\text{conf}} = (\pi/2)^{3/2} \cdot \omega_o^2 z_o = (1/2)^{3/2} \cdot V_{\text{eff}}$. Data were collected on a Zeiss LSM 510-ConfoCor 3 equipped with avalanche photodiodes (APDs) and LD C-Apochromat 40 × /1.1 NA water immersion objective. The laser was reflected by a 488/561 dichroic mirror onto the sample and the emitted fluorescent signals were filtered with a 505- to 540-nm bandpass filter during acquisition. One hundred 256 × 256 images (50 nm pixel size) were acquired with 12.79 μs pixel dwell time and 7.656 ms line time. Image analysis was performed using ZEN software (FCS/PCH) or SimFCS (RICS/N&B).

dividing the average count rate by the recovered particle number or from the fitted PCH curve. It is apparent that the molecular brightness of EGFP is stable from 20 to 160 nM and similar brightnesses are obtained whether FCS or PCH data are used (6123 and 6703 cpsm, respectively). However, brightness values became unstable at EGFP concentrations <20 nM, falling to about half the average values at 2.5 nM [2825 cpsm (FCS) and 3994 cpsm (PCH)]. A similar trend was observed for EGFP brightness values measured by N&B analysis [20 to 160 nM, 3723 cpsm; 2.5 nM, 1385 cpsm, Fig. 2(b)]. The same laser power was used for FCS/PCH and N&B measurements, but the N&B values are lower because of the reduced laser exposure time, due to raster scanning, that the EGFP molecules experience as the laser scans across the sample. Based on these titration experiments, we set the lower sensitivity limit at 20 nM for our system [see dotted vertical line in Figs. 2(a) and 2(b)]. For our Zeiss microscope setup, we observed poor recovery of brightness values using FCS and PCH methods if our signal count rate dropped below 10 kHz even though our background signal for the buffer alone was ~0.3 kHz.

Both FCS and PCH analytical models assume that the confocal volume is three-dimensional (3-D) Gaussian and has no distortions. We acquired a 3-D image stack of a 0.17-micron AlexaFluor 488-labeled bead to confirm that our confocal volume has a Gaussian distribution in the *X*-*Y* and *Z* planes (Fig. 3). We also calculated the EGFP diffusion coefficient by using the FCS data or performing RICS on the image series as a second test to confirm that we had not saturated the illumination volume. The average diffusion rate obtained was 109 and 92 $\mu m^2/s$ for FCS and RICS, respectively [line in Figs. 2(c) and 2(d)]. These rates are in good agreement with the generally accepted rate of ~90 $\mu m^2/s$ for EGFP in solution at room temperature.[51] If the illumination volume had been saturated, we would expect the volume to be non-Gaussian and the equations used to fit the autocorrelation functions would return diffusion values significantly different from 90 $\mu m^2/s$ because the fitting equations assume a Gaussian observation volume.

We plotted the recovered concentration of EGFP in solution as a function of nominal concentration (measured by absorbance) to determine the ability of FCS and RICS analyses to precisely measure concentrations [Figs. 2(e) and 2(f)]. Concentrations measured by both methods were determined using either the effective volume or confocal volume in the calculation. Concentration calculation using the effective volume returned values almost identical to the absorbance readings. In contrast, the concentrations calculated using the confocal volume, determined from fluorescent bead measurements, were very similar up to 80 nM and then deviated strongly at the highest EGFP concentration (160 nM). This underestimation of concentration above 100 nM for RICS has been reported previously.[43] The underestimation of values could be due to one of several reasons: (1) differences in the method of volume measurement (solution versus bead attached to slide), (2) nonfluorescent or aggregated protein, (3) adsorption to the chamber surfaces over time, or (4) due to small deviations in Gaussian shape (less likely). Regardless of the exact reason for this underestimation, both FCS and RICS can reliably measure concentrations up to 100 nM (count rate ~50 kHz) using our microscope setup, similar to a previous report,[43] and recovered values deviated by 20 to 50% at count rates >50 Hz. We conclude that a signal-to-noise ratio (SNR) of at least 10:1 is required for our avalanche photodiode (APD) detectors, concentrations up to 100 nM can

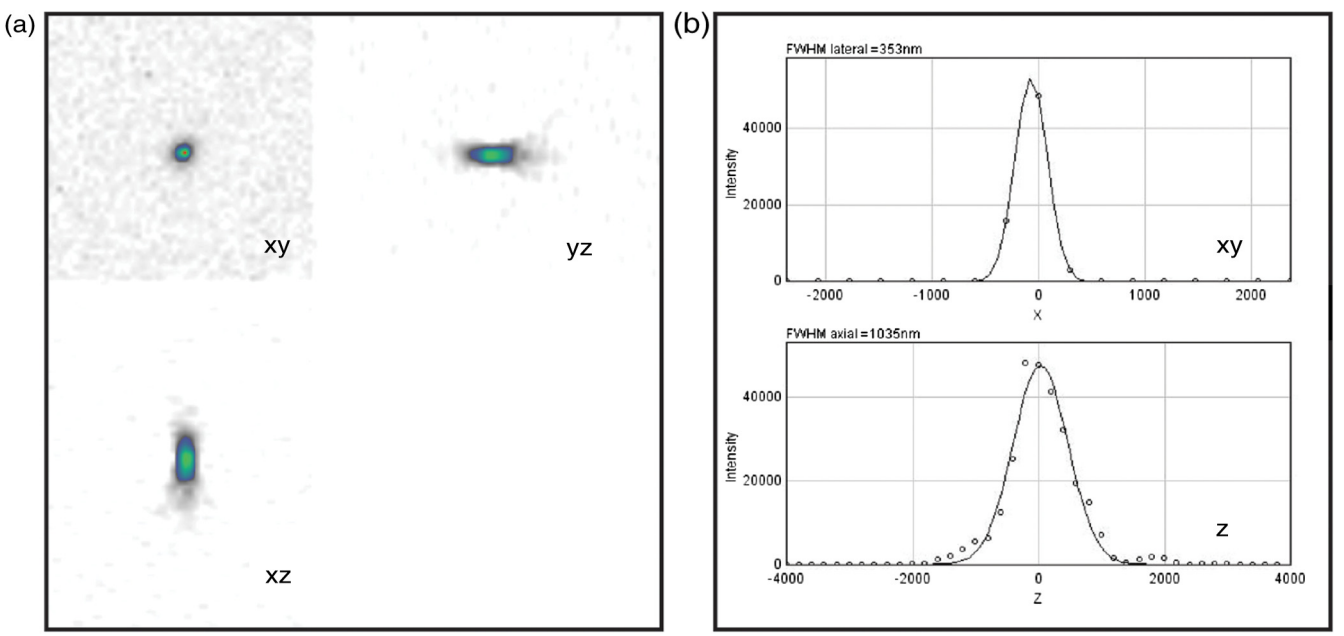

Fig. 3 Representative point spread function (PSF) measurement to confirm Gaussian illumination intensity profile. (a) The intensity profile of the PSF measured from a 0.17 μm fluorescent bead using a 40 × /1.1 NA water immersion objective. PSF is derived from a Z-stack of 100 images (256 × 256 pixel frame with z-step of 200 nm, pixel size of 296 nm, pixel dwell time of 12.8 μs and 1 Airy unit −78 μm), acquired on Zeiss LSM 510-ConfoCor 3. (b) The fitted curve (solid line) on the measured data points (open circles) demonstrating Gaussian profile with FWHM lateral axis = 353 nm and FWHM axial = 1035 nm dimensions giving a structural parameter of 2.93 and a confocal volume of 0.72 fl. All PSFs were generated and analyzed in ImageJ using the macro "MIPs for PSFs All Microscopes."[49]

be reliably measured, and the proper SNR and sensitivity should be determined for your microscope system.

3.3 *Determination of Optimal Laser Power Range*

We chose the lower sensitivity limit (20 nM) to conduct power series experiments in order to determine an optimal laser setting for FFS measurements. Brightness values recovered by FCS and PCH methods plateaued at 8.1 μW laser power. There was a sharp decline in brightness values at laser settings >8.1 μW, indicating saturation of the illumination volume [Fig. 4(a)]. This saturation was confirmed by an initial rise and then a sharp decline in recovered diffusion coefficients as laser power was increased from 8.1 to 16.5 μW (at the sample level) due to photodynamic processes [bleaching and flickering, Fig. 4(c)]. From 0.45 to 8.1 μW, the brightnesses increased linearly and FCS measurements should be kept in this linear range, preferably at the lowest setting possible. The maximum laser attenuation setting for FCS and PCH methods is 8.1 μW for our microscope setup [dotted vertical line, Figs. 4(a) and 4(c)]. In contrast, the N&B method has a greater dynamic range with a linear increase in brightness values recovered from 0.45 to 16.5 μW [Fig. 4(b)]. This observation is confirmed by the stable diffusion coefficients recovered across the entire range of power settings tested [Fig. 4(d)]. The upper power limit for measurements could be lower inside cells, but it is not always practical to do power series measurements inside cells due to the multiple variables that could affect the brightnesses. A rule of thumb is to determine the upper laser power setting in a defined environment, such as using purified components *in vitro*, and then set the laser power to 1/10 the limit for experiments. The upper limit in our case was 8.1 μW, therefore, we chose to set the laser attenuation to 0.45 μW (>1/10 the limit) for our cellular measurements. In most circumstances, this conservative setting will prevent illumination volume saturation and photobleaching during measurements. For molecules with very slow diffusion rates

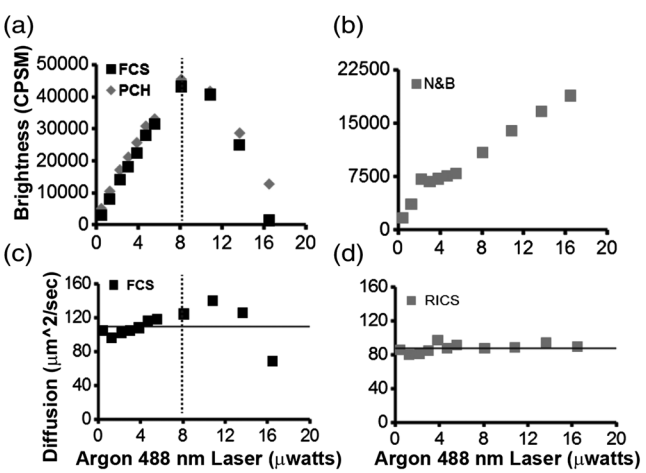

Fig. 4 Determination of optimal laser power for FFT measurements. The laser power was varied from 0.45 to 16.5 μW at the sample level of the 30-mW argon laser. The EGFP solution was set at 20 nM. (a) Plot of molecular brightness as a function of the laser power, measured using either FCS (black squares) or PCH (gray diamonds) methods. (b) Plot of molecular brightness as a function of the laser power based on N&B analysis. (c) and (d) Recovered diffusion coefficients as a function of laser power using FCS or RICS analysis, respectively. All Zeiss LSM 510-ConfoCor 3 settings are the same as in Fig. 2 with the exception of the laser power.

(e.g., membrane proteins), the laser power should be scaled to the residence time ($\sim 1/D$) in the detection volume because the "1/10" rule may not be sufficient to prevent bleaching. This can be difficult to do when the sample is very heterogeneous because of multiple species that have different diffusion rates, but scaling power based on diffusion should be done whenever feasible. Importantly, the same laser power must be used in order to compare brightness measurements between samples. In our experience, 0.45 to 2.46 μW laser attenuation settings work reasonably well for measuring the dynamics of many cellular proteins. For our system, setting the attenuation <0.177 μW usually results in unreliable power output.

FFS measurements can be performed on experimental samples once the detector sensitivity, illumination volume shape, and power range have been determined for your microscope system. It is also important to be vigilant for system instabilities, such as stage drift due to thermal variations, or mechanical or optical misalignments. Other sources of variation that can lead to artifacts in measurements are cellular movements, photobleaching of slowly moving molecules, and sample thickness bias (see Sec. 3.4).

3.4 *Discrepancy Between Brightness Values Measured In Vivo*

Recent *in vitro* and *in vivo* studies have concluded that calculation of molecular brightnesses using FCS, PCH, and other single point FFS measurements are equivalent.[5,6,29] However, photobleaching was observed in the studies performed on membrane proteins in cells, which could lead to an underestimation of the molecular brightness.[5,6] Photobleaching is common for membrane proteins even when the laser power is carefully controlled because of the slow diffusion (1 to 0.1 $\mu m^2/s$) and the confinement to a two-dimensional (2-D) membrane. We performed measurements on a cytosolic protein (EGFP), a subunit of focal adhesion complexes (Paxillin), and a membrane-associated protein [EGFP-glycosylphosphatidylinositol (GPI)] to determine if brightness values obtained from different methods are indeed equivalent *in vivo*.

HeLa cells expressing low levels of EGFP, EGFP-Paxillin, and EGFP-GPI were used for brightness measurements [Figs. 5(a1), 5(b1), and 5(c1)]. We define low levels of expression as cells having count rates of 150 kHz or below corresponding to nanomolar-to-micromolar concentrations. A z-scan was performed to position the illumination volume in the center of the fluorescently labeled cellular structure or cellular membrane depending on the protein being measured. Ten scans of 10 s were performed for each protein and the FCS/PCH curves were fitted (see protocols 1 and 2 for FCS and PCH). After FCS and PCH data collection, a stack of 100 images were collected for N&B analysis (see protocol 3 for N&B). The FCS and PCH experimental data fit well to a single component model as seen by the tight distribution of residuals [Figs. 5(a2), 5(b2), and 5(c2)]. The molecular brightness values for cytoplasmic EGFP were similar regardless of the method used [3730, FCS; 5309, PCH; 3920, N&B Fig. 5(a3)] or the microscope system used [4145, Leica TCS SP5 (data not shown)]. We also routinely measure the brightness of a tandem-EGFP protein (EGFP-linker-EGFP) to calibrate our brightness scale and the brightness is roughly twice that of EGFP, confirming the precision of our experimental setup (data not shown).

In contrast, there was a discrepancy in the brightness measurements for EGFP-Paxillin and EGFP-GPI. The average N&B

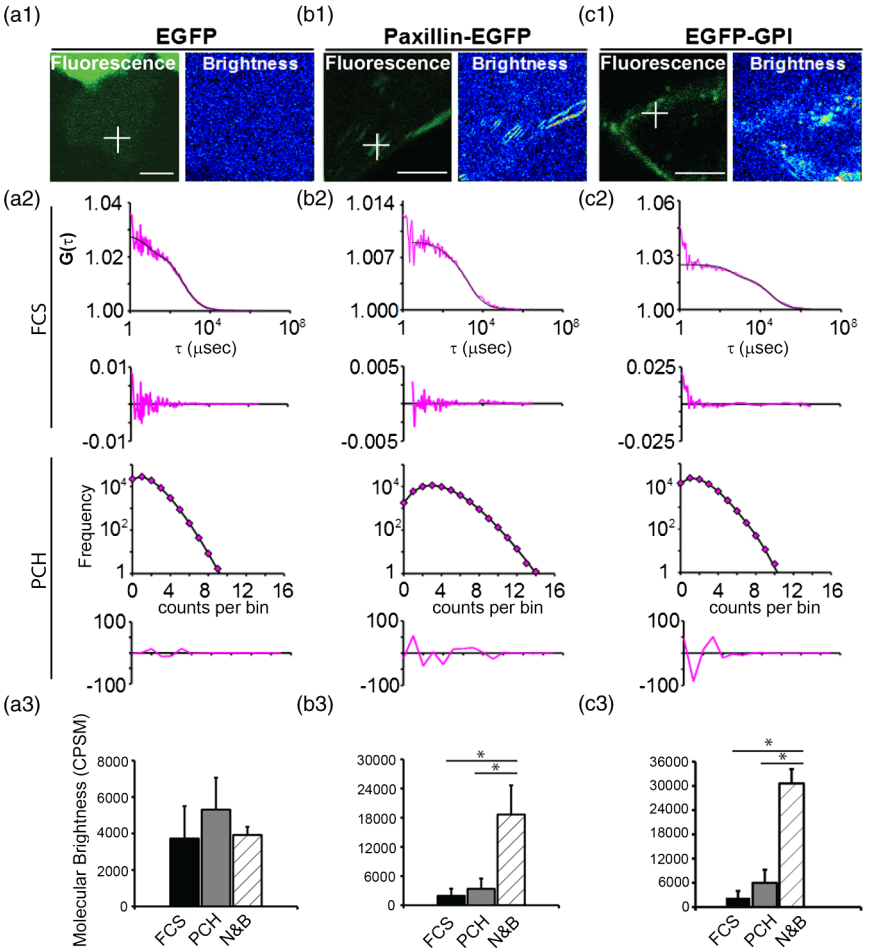

Fig. 5 Discrepancy between molecular brightness values for FCS, PCH, and N&B analyses in cells expressing EGFP-Paxillin or EGFP-glycosylphosphatidylinositol (GPI). (a1), (b1), and (c1) Fluorescence images of HeLa cells expressing EGFP, Paxillin-EGFP, or EGFP-GPI; scale bar = 10 μm (EGFP), 5 μm (Paxillin-EGFP, EGFP-GPI). Crosshair indicates position of FCS/PCH measurement. Molecular brightness B maps were generated in SimFCS software. (a2), (b2), and (c2) Representative FCS curve and PCH histogram for EGFP, Paxillin-EGFP, or EGFP-GPI. The raw data are plotted in pink and the fitted curve is black with corresponding residuals below. FCS correlation curves were averaged from several 10-s scans to obtain better statistics. Bin time was 50 μs for PCH data analysis. Data were collected on the Zeiss LSM 510 META ConfoCor 3 system. (a3), (b3), (c3) Cytosolic EGFP molecular brightness is plotted as CPSM measured by FCS ($n = 7$ cells), PCH ($n = 7$ cells), and N&B analysis ($n = 7$ cells). Paxillin-EGFP molecular brightness is plotted as CPSM measured by FCS ($n = 10$ cells), PCH ($n = 10$ cells), and N&B analysis ($n = 7$ cells). EGFP-GPI molecular brightness is plotted as CPSM measured by FCS ($n = 4$ cells), PCH ($n = 5$ cells), and N&B analysis ($n = 4$ cells). Unpaired t test, $^*p < 0.05$ (N&B versus PCH), $^*p < 0.05$ (N&B versus FCS). Errors are standard deviation. FCS, PCH, and N&B data are pooled from two experiments and analyzed using ZEN software (FCS/PCH) or SimFCS (N&B).

brightness value for EGFP-Paxillin was 18,664 cpsm compared to ~1950 and ~3383 cpsm for FCS and PCH measurements, respectively [Fig. 5(b3)]. If we normalize our N&B brightness values, then we obtain an average of ~6.63 Paxillin molecules (range 2.9 to 9.3) dissociating from adhesions, which is in good agreement with previous N&B studies that found complexes ranging in size from 6 to 10 molecules.[16] We also observed a discrepancy if we measure the brightness of the membrane anchored protein EGFP-GPI using FCS and PCH, versus N&B analysis [2287, FCS; 5978, PCH; 30,602, N&B Fig. 5(c3)]. The EGFP-GPI brightness values obtained by N&B analysis correspond to roughly five to eight molecules per cluster, which is similar to a recent study investigating the clustering of EGFP-GPI in a cell model of Fabry disease.[52]

We believe one reason for this discrepancy between the spot measurements (stationary laser beam) and the raster scanning approach is due to more photobleaching in the 10-s illumination time on a fixed spot versus 25 μs dwell time on a pixel of an image frame. For both EGFP-Paxillin and EGFP-GPI, during several measurements, there was apparent photobleaching that occurred during the first 10-s scan that most likely represents slow-moving complexes being bleached (Fig. 6). Elegant studies using a combination of scanning FCS (sFCS) and RICS identified a heterogeneous dynamic behavior for Paxillin in cells.[53] Based on these studies, monomers of Paxillin are thought to bind to quasi-immobile structures during adhesion assembly and large aggregates are released during disassembly.[53] In the study, Digman et al. used a two-component model to fit their

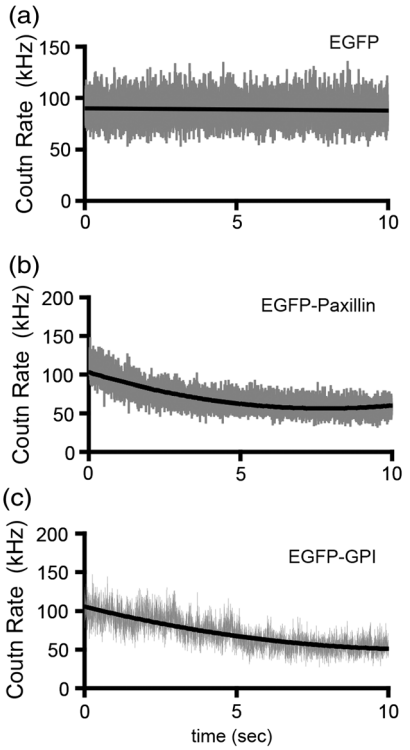

Fig. 6 Photobleaching is partially responsible for underestimation of molecular brightness values for EGFP-Paxillin and EGFP-GPI using FCS/PCH methods. A representative photon count trace, measured with FCS, from EGFP in cytoplasm (a), EGFP-Paxillin in focal adhesions (b), and EGFP-GPI in plasma membrane (c). First trace of 10 shown. Note the photobleaching that was seen in a majority of cells expressing EGFP-Paxillin and EGFP-GPI measured but not EGFP. The photobleaching was seen in the first scan but not in subsequent scans and most likely represents bleaching of slowly moving large oligomeric species that can be detected by N&B analysis (see Fig. 5). Traces are fitted with trend lines to illustrate the decay of the intensity trace for EGFP-Paxillin and EGFP-GPI but not for EGFP.

data. Fitting our PCH data for EGFP-Paxillin to a two-component model did not yield a better fit (data not shown).

This bleaching of EGFP-GPI during our FCS measurements has been observed by others.[54] It is apparent that the bleaching subsides by the end of the scan and, indeed, subsequent scans[2–10] are free of bleaching artifacts and these scans were used for analysis. The subsidence of the bleaching is most likely due to the complete bleaching of slow-moving/immobile species. In some instances, a visible bleached spot can be seen after acquisition. For our analysis, we left out the first scan and we believe this is leading to the underestimation of the molecular brightness for EGFP-Paxillin and EGFP-GPI using FCS/PCH methods because the large bleached species appear to be invisible during subsequent scans and are not replenished during the acquisition time frame. It is possible to correct for photobleaching and this has been accomplished in some instances.[55,56] However, the full nature of the photobleaching must be characterized in order to correct for it, which is not always trivial. Paxillin clusters were detected using sFCS where the laser beam is moved across the sample, thus minimizing bleaching.[53]

Molecular brightness can become artificially inflated when the cell thickness falls below a critical value (<2 μm; Ref. 29). This occurs because most mathematical models used to fit FFS data assume a finite uniform geometry that becomes confined and distorted as the sample thickness decreases due to a higher density of fluorescent molecules occupying the center of the volume. We were careful to choose cell areas for a measurement that were not too thin (>2 μm), therefore, this is an unlikely reason for the discrepancy in brightness values. Regardless of the exact reasons for the discrepancy, it is clear that relying on one brightness method to determine oligomeric status of a protein from brightness measurements is not optimal, especially if photobleaching cannot be accurately corrected.

3.5 *Summary and Recommendations*

In this tutorial, we review several different methods for determining molecular brightness values for fluorescent molecules. The basic theory for FFS measurements is provided along with the advantages and disadvantages of the particular methods. It is critical to properly calibrate and characterize your microscope system before performing actual experiments. We suggest performing concentration and laser power series experiments to determine the lower sensitivity limit and the optimal laser power, respectively. It is also important to characterize the shape of the illumination volume since the mathematical models for FFS techniques assume 3-D Gaussian profiles. If the volume is not 3-D Gaussian due to sample bias, the models can be modified to accommodate the altered shape.[29] Performing this shape check is also valuable for confirming that the instrument optics are properly aligned and free of damage. Oil-immersion objectives have focal-depth dependences that can lead to distorted brightness values. Therefore, we recommend using water-immersion objectives that have a collar to correct for coverglass thickness and do not have depth distortions. Detector characteristics, such as deadtime and afterpulsing, can impact measurements, but this can be minimized if the signal intensities are kept well below saturation levels (1/100 to 1/1000) and the fluctuations being studied are not on the same time scale as the detector traits. Detector deadtime and afterpulsing have to be corrected if fast chemical processes are being studied.

Similar brightness values can be recovered independent of the FFS method used for well-defined systems *in vitro*.[29] However, we demonstrate that for heterogeneous systems *in vivo*, this is not always true. The discrepancy in brightness values between methods can be partly linked to photobleaching of a subpopulation of the molecules due to the slower diffusion kinetics. Therefore, caution should be exercised when using only one brightness technique to infer the oligomeric status of a protein in cells and we argue, similar to several groups,[29,53] that several complementary techniques should be employed and compared.

Table 1 lists our recommendations for instrumentation requirements/settings based on our experience using a Zeiss LSM microscope system and can be used as a reference for other microscope systems. It is important to select cells expressing as low a fluorescent signal as possible but still maintaining a good SNR (e.g., 10:1) for FFS measurements. We provide general protocols to perform FCS and PCH measurements that can be used with commercial or home-built microscope systems. We also provide a protocol for N&B analysis employing the SimFCS software that can be used with data collected from commercial confocal microscopes (e.g., Zeiss, Leica).

FFS techniques are robust and sensitive when the microscope system is properly calibrated and aligned. Importantly, care should be taken when interpreting FFS data for membrane or membrane-associated proteins in living cells due to the

Table 1 Recommended equipment and settings for fluorescence fluctuation spectroscopy measurements.

Parameter	Type or range of values
Confocal microscope	Equipped with correlator card and associated electronics
Objective type	High NA (1.1 or greater), preferably water-immersion
Objective magnification	40×, 63×, or 100×
Laser	Appropriate wavelength for fluorophore (e.g., argon laser for EGFP)
Filters	Appropriate dichroic filters and bandpass for fluorophore (e.g., 488-nm dichroic and 505 to 540-nm bandpass for EGFP)
Pinhole	0.8 to 1 AU (1 AU ~78 μm for 488 nm wavelength)
Detector	Avalanche photodiode or hybrid [higher sensitivity and less noise than photomultiplier tube (PMT)]

Note: EGFP, enhanced green fluorescent protein.

increased possibility of photobleaching and, thus, incorrect estimation of recovered parameters, such as molecular brightness. We hope that this tutorial containing practical advice and protocols will be of use to those routinely using FFS techniques and the wider scientific community, especially those persons interested in implementing these powerful techniques in their own laboratories.

Protocol 1—FCS Protocol to Measure EGFP in Solution or Mammalian Cells

Materials

Reagents

1. 20 to 40 nM purified EGFP (Biovision, Milpitas, California, catalog #4999-100) or a different purified fluorophore; make sure appropriate filters and laser lines are available before continuing.
2. 25 mM Tris pH = 8.0 or phosphate buffered saline (PBS) +1% bovine serum albumin (BSA) for dilution of EGFP stock from Biovision
3. Dulbecco's modified Eagle's medium (DMEM) with phenol red (Sigma, Saint Louis, Missouri, catalog #D5796) for culturing HeLa cells
4. Minimum essential medium (MEM) Eagle without phenol red (Sigma, catalog #M3024) +25 mM Hepes pH = 7.3 + 2 mM L-glutamine
5. Fetal bovine serum (FBS, Gemini Bioproducts, catalog #100-106)
6. Penicillin-Streptomycin (Sigma, catalog #P0781)—optional
7. Cultured HeLa cells or cell line of choice
8. Rat tail collagen type I (Millipore, catalog #08115)
9. Live cell dishes 0.17 glass-bottom dish (Bioptech, catalog #04200417C)
10. Lipofectamine 2000 transfection reagent (Invitrogen, catalog #11668-019)
11. Plasmid containing EGFP or EGFP-fusion protein

Equipment

1. Commercial (e.g., Zeiss, Leica-SMD, PicoQuant-LSM Kit) or home-built microscope system equipped with hardware and software for correlation analysis
2. LD C-Apochromat $40\times/1.1$ NA water-immersion objective
3. APD detectors or other high-sensitivity detectors, such as hybrid or single-photon avalanche photodiode for FCS/PCH measurements
4. PMT detectors (for capturing images of cells)
5. Environmental chamber to maintain temperature, CO_2 level, and humidity. We use a live cell environmental chamber made by Pathology Devices Inc. (Westminister, Maryland).
6. Software to analyze data (e.g., IgorPro, MATLAB®, SimFCS, FFS data processor, SymPhoTime 64)

Procedure

Reagent setup

- Grow HeLa cells in DMEM + 10% FBS (antibiotics optional) in a 37°C humidified incubator with 5% CO_2 (or your cell of choice in appropriate growth media)
- Coat Bioptech dish (or MatTek) with 1 ml of ~60 μg/ml type I collagen (diluted from stock with 0.02 N acetic acid) for 15 to 20 min at room temperature. Rinse dish twice with growth media.
- Seed 150,000 to 200,000 HeLa cells into type I collagen coated Bioptech live cell dishes two days before experiment.
- Transfect cells with appropriate plasmid the day before the experiment using Lipofectamine 2000. Usually 50 to 200 ng of plasmid is sufficient to obtain a protein expression level amenable for FFT measurements. We also recommend using ~1/4 less lipofectamine reagent as suggested by manufacturer to lower expression and reduce vacuoles. For example, we routinely use a 2:1 or 3:1 (μl/μg) reagent to DNA ratio. Normally, we express the protein for 12 to 16 h but can see weak expression as early as 8 h with a cytomegalovirus promoter.
- Next day, change growth medium to MEM without phenol red supplemented with 2 mM L-glutamine, 25 mM Hepes pH = 7.3 plus 1 to 10% FBS. MEM without phenol red is prepared from powder ahead of time according to manufacturer's directions and can be stored for several

weeks at 4°C away from light. You can also use PBS buffer in place of growth media minus phenol red if measurements are to be done quickly (1 h or less).

Equipment setup

- Turn on microscope and associated accessories.
- Open microscope operating software, turn on desired laser lines (argon laser for EGFP) and set tube current to 6.1 A. Make sure laser is on for 1 h before starting experiment.
- Turn on environmental chamber and equilibrate to 37°C or desired temperature for experiment with 5% CO_2 and humidified air. EGFP solution measurements can also be performed at room temperature.

Measure EGFP in Solution

1. Place a drop of high-purity water (e.g., Millipore 18 MΩ) onto water-immersion objective and then dish containing 20 to 40 nM EGFP in PBS+1% BSA solution on the stage
2. Turn on the laser line(s) needed for experiment. In this case, it is 488-nm line.
3. Set up and turn on environmental chamber (if needed) and let system warm up for ~1 h.

Coverglass thickness measurement

1. Attenuate laser power to 1 to 2% of output for 488-nm line of argon laser, set 80/20 neutral filter as the main dichroic mirror, mirror(s) for the secondary dichroic, and no emission filter to the PMT detector.

   Light path = Laser > 80/20 neutral filter > mirror (s) > none(no emission filter) > PMT detector

   Note: It is better to use the PMT detector instead of the APD for the coverglass thickness measurement because the amount of reflected light could more easily damage the more sensitive APD.
2. Set acquisition to line scan mode and scanner speed to max.
3. Set pinhole to maximum, Gain to 200 to 400, or appropriate setting not to saturate PMT.

   Note: However, if the APD is used for coverglass thickness measurements, then reduce the pinhole diameter and gain so as not to saturate/damage the APD.
4. Start continuous scanning and focus toward the dish to find the bottom and top of the coverglass.
5. When the objective is focused at the bottom of the coverglass, the signal intensity line will deflect up [Figs. 7(a) and 7(b)]. Make note of the Z-position at the first deflection and then continue to focus up till a second deflection occurs; this is the top of the coverglass.

   Note: When the focus is in the glass, the scanning line comes down; when the focus is at the top of the glass, the line deflects up again. If a scanning line option is not available, then frame imaging can be used and the change from a dark image to a bright white image will be apparent.
6. Subtracting the first deflection Z-focus position from the second will give the coverglass thickness. The thickness value recovered from this method is not the true value and must be corrected due to the refractive index mismatch (water versus glass).

   Correction for water-immersion objective: $\text{Thickness}_{\text{corr}} = n_{\text{glass}}/n_{\text{media}} \times$ measured thickness.
   Example: $1.518/1.333 \times 150 = 1.14 \times 150 = 0.171$ μm.
7. Adjust the objective collar to 0.171. Many water-immersion objectives have two marks for setting the correction, usually a red line (used for 37 deg) and a black line (used for room temperature). If your objective has only one mark, then use this mark.
8. Focus ~200 μm above the top of the coverglass to avoid interference from the glass and position the confocal volume fully into the sample.
9. Set the following light path for FCS measurements. Note that this is the light path used for FCS/PCH acquisition.

   Light path = Laser > 488/561 dichroic > mirror(s) > 505 to 540 band pass filter (or equivalent) > APD detector

   Note: Attenuate 488-nm line power (0.3 to 0.5%) for measuring EGFP in solution and the detector has been switched from PMT to APD for FCS/PCH measurements.
10. Inspect the count rate (intensity as function of time) and do not exceed 1 MHz (ideally should be <200 kHz). Count rates of 20 to 200 kHz are appropriate for

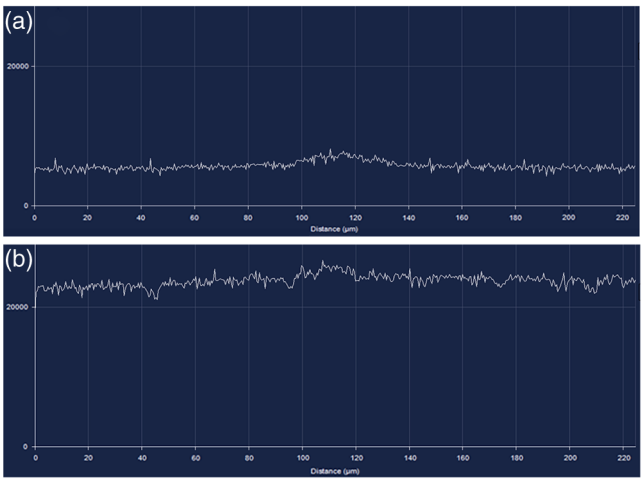

Fig. 7 Line scan mode window in Zeiss ZEN software (version 2008). (a) Intensity plotted as a function of pixel distance for reflected light from the bottom surface of a live cell dish. (b) Intensity plot from (a) after focusing on the coverglass bottom of the dish. Note the jump in the intensity line. From this point, moving the objective up lowers the line, and then the line jumps the second time (not shown here). The distance between the jumps of the line scan can be used to measure coverglass thickness.

measuring samples and should be well below the saturation of the confocal volume. Intensity levels can also be monitored if the count rate is not available. For each system, the saturation level must be determined empirically.

Note: Saturation of the confocal volume will lead to an apparent increase in the detection volume and underestimation of the diffusion coefficient.

11. Set the pinhole size to 1 AU for the APD. Below is the pinhole size in microns for several common wavelengths.

    Pinhole size (μm, λ in nm): 66, 458; 70, 488; 74, 514; 78, 543; 90, 633

12. If allowed, adjust pinhole in X and Y directions to maximize the amount of light directed into the APD detector (e.g., Zeiss and ISS systems).

    Note: Some microscope systems, such as Leica SMD-FCS, have automated the pinhole alignment process, therefore, no user intervention is needed.

FCS measurement for sample in solution

1. Once count rate (intensity level) is in an acceptable range and the pinhole is set, start an FCS measurement of the GFP in solution.

   Note: For GFP and other fast-moving molecules in solution (e.g., small fluorescent probes), a single scan of 100 s will suffice for data analysis. If for some reason photobleaching occurs, then multiple shorter scans can be employed, such as 10 scans of 10 s each. This method is usually employed for FCS measurements of molecules in live cells because the diffusion rates are slower and the molecules are prone to bleaching. However, longer scans are preferable to shorter scans for improving statistics (SNR).

2. Example of FCS data for 30-nM EGFP in solution (Fig. 8).

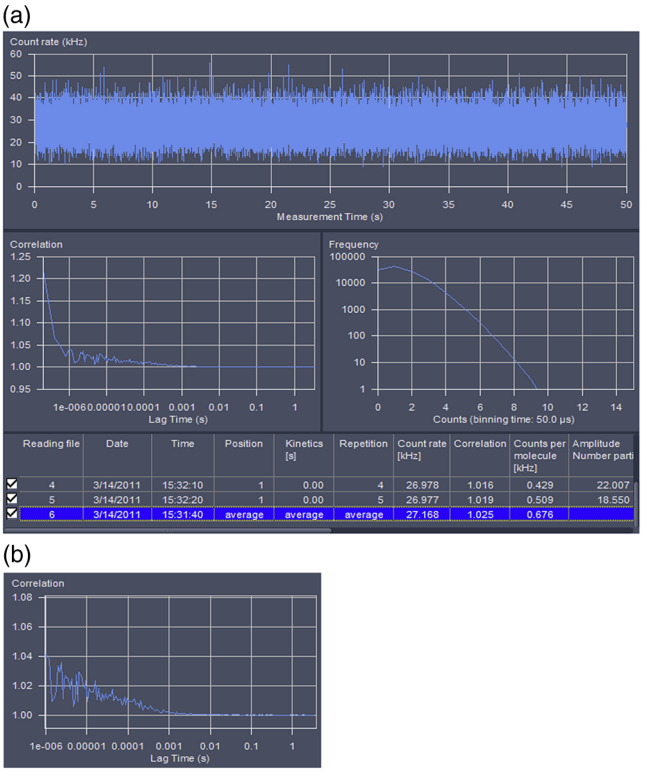

Fig. 8 Example FCS and PCH data for GFP in solution. (a) Window in Zeiss ZEN software showing count rate plot, autocorrelation curve, and PCH for 30-nM GFP in solution. (b) Autocorrelation curve after removal of time points due to afterplusing.

See Sec. 4.4 for details on how to fit data to obtain diffusion coefficient and how to calibrate volume.

Controls to run

- No laser—to measure shot noise
- Buffer only—to determine the background signal from the buffer or any buffer additive present in the sample (e.g., BSA, salt, or detergent)
- Each fluorescent molecule alone in buffer for dual-label experiments

Measurement of EGFP Expressed in Mammalian Cells

1. Turn on microscope, laser, and other required accessories as needed (e.g., environmental chamber, CO_2). Let system warm up for ~1 h.

2. Place a dish containing cultured HeLa cells, or another appropriate cell line, transfected with EGFP in cytoplasm on the microscope stage in the environmental chamber (37°C, 60 to 65% humidity, 5% CO_2).

3. Determine thickness of dish coverglass following the steps in Coverglass thickness measurement under Measure EGFP in Solution section above.

   Important: Do not focus 200 μm above the top of coverglass this time because we will be manually focusing on cells.

4. Adjust correction collar to dish thickness.

5. Set the light path to detect GFP fluorescence in confocal mode. Set the pinhole to ~3 AU (220 to 250 nm) to more easily identify weak-expressing cells. Set master gain for PMT detector to 500 to 750 and laser power to 0.3 to 0.5% (same as used for EGFP in solution). Zoom can be set as 1 to 3.

   Light path = HFT 488/561 > mirror(s) > filter 505 to 540 band pass – PMT detector.

   Note: PMT detector is used first to identify the low-expressing cells and not APD because if a very bright cell is in the field of view during scanning, this could damage the APD even if the safety shutoff is triggered. It is safer to use the less sensitive but broader dynamic range of the PMT.

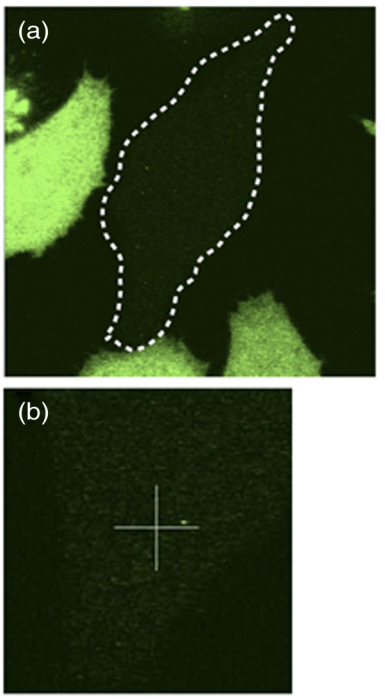

Fig. 9 Representative confocal image of EGFP expressing cell. (a) HeLa cell expressing low levels of EGFP amenable for FCS measurements surrounded by high expressing cells. Dotted line depicts boundary of the cell. (b) Zoom in the cytoplasm of the cell. Crosshair indicates where FCS spot measurement was made.

6. Figure 9 illustrates an example of a mammalian cell with weak expression of GFP surrounded by higher-expressing cells.

7. Once a suitable cell is identified, perform a Z-scan in FCS mode to determine the thickness of the cell. The confocal volume should be positioned in the middle of the structure where the measurement is to be done. If possible, areas of the cell <2 μm thickness should be avoided to prevent sample thickness bias.

   Note: In this case, the middle of the cytoplasm is selected to maximize the signal. If a membrane protein was being investigated, then the volume should be positioned in the middle of the membrane and the resultant FCS data should be fitted with a two-dimensional Gaussian model (see Analysis section).

8. Several microscope systems employ a cross-hair for picking where to make a measurement [see Fig. 9(b)]. If a cross-hair selection is not available, then use another available method to focus on the spot of interest (e.g., zooming in or selecting ROI).

9. For acquisition of FCS/PCH data, switch light path to APD (see steps 9–12 in Coverglass thickness measurement section), set the scan time and number of scans, and then start the acquisition.

   For acquisition on a second cell, repeat steps 6 to 10 in this section.

10. Save file for later analysis. If microscope system does not have analysis software, then export the raw data for use in third-party software (e.g., SimFCS, FFS data processor, SymPhoTime 64). Also, save a copy of the confocal image showing where the measurement was taken for documentation.

Note: Acquisition settings

The scan time should be at least 1000 times longer than the diffusion time (τ) of the molecule under investigation. For proteins expression in the cytoplasm, 10 s is usually sufficient. For membrane proteins, longer scan times, such as 25 to 100 s, are needed. For statistical purposes, performing one long scan is better than several shorter scans (e.g., 1×100 s versus 10×10 s) because it improves the SNR. This is not always achievable when making measurements inside cells due to photobleaching. Usually, a compromise is made where 7 to 10 scans of 10 to 25 s are performed. Averaging these scans together gives statistics similar to one long scan. If photobleaching is a problem, then reduce the measurement time and increase repetitions. If the signal is too strong (e.g., >200 kHz), then a pre-acquisition photobleach of the selected region can be performed.

Note: Choice of fluorescent probes

If a fluorescent protein or dye other than EGFP is used, then change the dichroic mirror and filters accordingly. It is also important to make sure the probe does not have a high triplet state fraction under the laser excitation conditions used. There is no consensus in the field and acceptable levels of triplet formation range from <10% to no >25%. The levels of triplet species should be kept as low as possible. The probe should also be bright and resistant to photobleaching. However, no fluorescent probe has all the desirable characteristics and compromises are sometimes made.

FCS Analysis

1. Open data file in analysis software. Any analysis software that allows user-defined fitting models and nonlinear regression can be used to fit the raw FCS data (e.g., IgorPro, SigmaPlot). There is also commercially available software, such as SymPhoTime 64 from PicoQuant, software licensed from academic institutions, such as SimFCS (Laboratory of Fluorescence Dynamics, UC Irvine, Irvine, California) and FFS Data Processor (Scientific Software Technology Center, Belarusian State University, Minsk, Belarus) that can be used.

2. The large dropoff in the autocorrelation curve which is at times faster than 1 μs is mainly due to detector afterpulsing [Fig. 8(a)] where an imaginary event is registered leading to a false positive correlation signal. This part of the curve should not be used in fitting the data for the diffusion time and number of molecules [start fitting ~1 to 10 μs, Fig. 8(b)].

3. Select/input an appropriate diffusional model to fit the autocorrelation curve. For example, a 3-D anomalous diffusion model for EGFP in the cytoplasm of the cell would be appropriate (see equation below). Other species under investigation (e.g., membrane protein) would require a 2-D model.

4. Analytical function for 3-D anomalous diffusion

$$G(\tau) = 1 + \frac{1}{N} \cdot \frac{1 - F + F_e^{(-\tau/\tau_f)}}{1 - F} \cdot \frac{1}{1 + (\frac{\tau}{\tau_D})^{\alpha} \cdot \left[\left(1 + \frac{1}{S^2}\right) \cdot \left(\frac{\tau}{\tau_D}\right)^{\alpha}\right]^{1/2}}.$$

The variables N, τ, $G(\tau)$, F and S represent the number of particles in the confocal volume, correlation time, autocorrelation function, fraction of molecules in triplet state, and the eccentricity or structural parameter ($S = \omega_z/\omega_{x,y}$), respectively.

Note: The geometric shape factor (γ) should be set to 0.350 for one-photon excitation and 0.076 for two-photon excitation, respectively. The structural parameter [the ratio of w_z to $w_{x,y}$ (focal shape)] can be set to a specific value based on the measurement of a free dye in solution. The structural parameter for our experiments was set to 3 to 5 based on measurement of a fluorescein dye standard or fluorescent bead measurements to calculate the PSF. It is important to keep the triplet fraction as low as possible to recover an accurate number of molecules (N).

5. Check to make sure the residuals for the fitted FCS curve are evenly distributed around the x axis and a chi square value close to 1.

6. Once the diffusion time is recovered from the fit, the diffusion coefficient can be calculated using the equation listed below:

$$D = \frac{\omega_{x,y}^2}{4 \cdot \tau_D},$$

where τ_D is the diffusion time (from the fit), D is the diffusion coefficient, and $\omega_{x,y}^2$ is the waist of the PSF measured either by performing an image series along the z axis on a diffraction-limited fluorescent bead (see Fig. 3) or measuring the diffusion of a dye with a known diffusion rate. For waist determination by free dye, the FCS curve is fitted to recover the diffusion and then the waist is solved because the diffusion rate is known ($\omega_{x,y}^2 = D \cdot 4\tau_D$).

The equation below is used with the average molecule numbers (N) recovered from the FCS curve fit to calculate the molecular concentration.

$$\text{Concentration} = \frac{N}{N_A} \cdot V,$$

where N_A is Avogadro's number and V is the focal volume. The effective focal volume (V_{eff}) can be calculated using the following formula:

$$V_{\text{eff}} = \pi^{3/2} S (4D\tau_D)^{3/2}.$$

S, D, τ_D parameters can be determined from the FCS measurement of free dye in solution. Note that if the laser power is changed, then the volume will need to be calculated again.

Typical values for the aforementioned parameters are listed below:

$\omega_{x,y} = 200$ to 400 nm
$\omega_z = 400$ to 1800 nm
S (also called k) $=2$ to 6
Volume $= 0.3$ to 1.2 fl

For our microscope system, the average confocal volume using fluorescent beads was 0.75 fl ($n = 10$) when excitation is 488-nm laser line.

7. Once N is known, an estimate of the molecular brightness can be determined by dividing N by the average count rate (k).

For additional information, see Ref. 54.

Protocol 2—PCH Analysis from Collected FCS Data

Materials

See protocol 1.

Procedure

See protocol 1.

Collection and Analysis of PCH Data

1. Follow the instructions in protocol 1 for measuring EGFP either in solution or in a cell to obtain fluorescence intensity traces as a function of time.

2. The same traces used to create the correlation curves for FCS can be used to generate PCHs. We normally analyze our data using the PCH fitting module in the Zeiss software ZEN. For those without access to ZEN software, raw traces can be analyzed using the freely available ImageJ plugin created by Jay Unruh at Stowers Institute for Medical Research in Kansas City, Missouri.[57] The following protocol demonstrates PCH analysis using the Jay Unruh ImageJ plugin.

3. Install the Unruh ImageJ plugins and open the PCH analysis tool under trajectory tools [Fig. 10(a)].

4. Input the sampling frequency, which is the bin time used to generate the PCH curve (e.g., 50 μs = 20,000 Hz). We normally acquire our data for cytoplasmic EGFP at 50 μs; therefore, we input 20,000. We also have used 20 μs bin time and obtained similar results.

Note: The bin time should be shorter than the diffusional time of EGFP for accurate PCH measurements. Perroud and colleagues suggest that the bin time should be 34% shorter than the diffusion time to keep the error in measurement <10%.[45] Practically, for cytosolic and membrane proteins, the bin time should be 20 to 50 μs and 100 to 150 μs, respectively. For measuring free fluorescent dyes in solution, the bin time should be set to 10 to 20 μs. Bin times <10 μs should be avoided because at these short times, triplet state

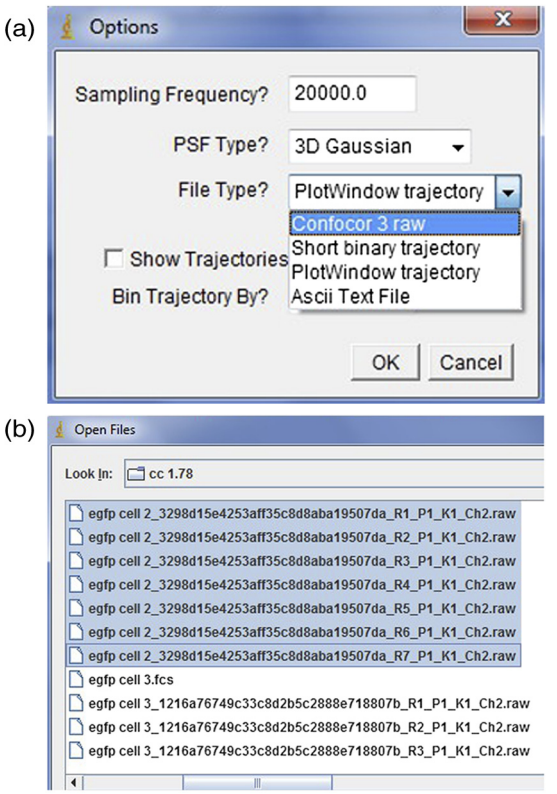

Fig. 10 Options and Open File windows in Unruh ImageJ plugin. (a) The sampling frequency, PSF type, and file type can be selected in the Options window. In this example, the ConfoCor3 raw file type is selected. (b) Single or multiple files (highlighted) can be opened in the plugin.

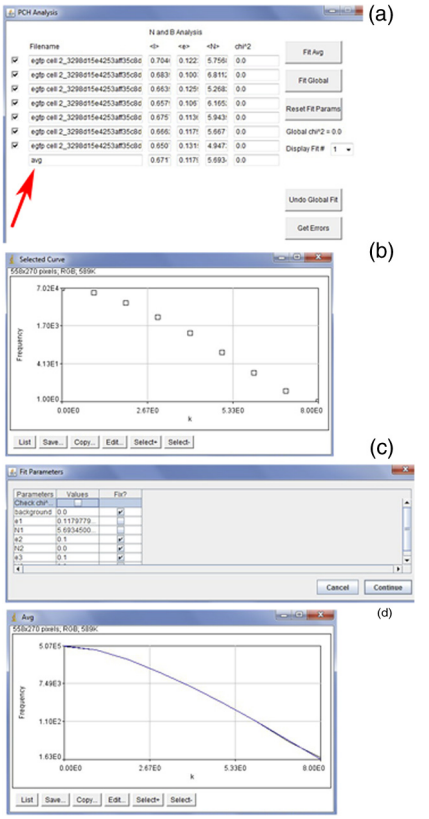

Fig. 11 PCH analysis and Fit Parameter windows in Unruh ImageJ plugin. (a) PCH analysis window displaying intensity (I), brightness (ε), number (N), and chi squared (chi^2) for selected files. Red arrow points to the average value for all scans. Buttons on the right side allow for average, or global fitting and resetting fit parameters. (b) Selected curve window showing the PCH plot for the average of all the scans. Buttons on bottom allow for List, Save, Copy, Edit, and Select for plot. (c) Fit Parameter window showing variables that can be set for fitting or fixed value. (d) Average PCH plot after fitting to one species model. The fitted data (blue line) is directly over top of the data points (black line).

formation and isomerization of the fluorophore greatly contribute to fluorescence fluctuations and the PCH. Characteristics of the photodetector, such as deadtime and afterpulsing, also contribute and must be corrected for very short bin times (<10 μs; Refs. 58 and 59).

5. Select the file type for the input file [Fig. 10(a)]. There is a choice of ConfoCor 3 raw file, short binary trajectory, plot window trajectory, and Ascii text file.

   Only select bin trajectory and set bin time if you want to display the intensity trace. This bin time is strictly for displaying the trace not the PCH curve.

6. Navigate to the folder containing the file, select it, and press open. Multiple files can be opened at once by pressing control and highlighting desired files [Fig. 10(b)].

7. Figures 11(a) to 11(d) depict the results of the N&B analysis for seven traces of EGFP in the cytoplasm of a mammalian cell. The results listed are the average intensity ($\langle I \rangle$), average brightness ($\langle e \rangle$) in counts per molecule (cpm), and average number of molecules ($\langle N \rangle$). Multiply $\langle e \rangle$ by the bin time in Hz (sampling rate) to convert cpm to cpsm (e.g., $0.117 \times 20{,}000 = 2340$ cpsm). Pressing the Fit Avg button will perform a nonlinear regression on the averaged PCH. Deselecting individual curves (left side of window) will remove that scan from the final fitting. A global fit can also be performed by pressing the Fit Global button.

8. Pressing the Fit Avg button opens the Fit parameters window [Figs. 11(a) and 11(c)]. Here the brightness (e), number (N), and background can be set to be fixed or variable depending on the parameter to be solved for. The background signal from nontransfected cells is usually 50- to 100-fold lower than the GFP signal and we usually set the background to zero.

9. The chi^2 for the fitted PCH curve should be close to 1.0, indicating a good fit. The plugin also displays the fitted curve over the data points [Fig. 11(b)] for comparison [Fig. 11(d), blue = fit, black = data].

   Note: The Unruh ImageJ plugin can also analyze two-color PCH and FCS data.

Protocol 3—N&B Image Collection and Data Analysis

Materials

See protocol 1.

Procedure

See protocol 1.

Acquisition of Image Series for N&B Analysis

(Note, > means open window in program. Image series acquired with the settings in this protocol can be used for both RICS and N&B analyses.)

1. Turn on microscope system as described in protocol 1 and let lasers/lamps warm up for 0.5 to 1 h.

   In our case, we acquired our image series on a Zeiss 510 Meta ConfoCor 3 system but any confocal microscope system with APD or photon-counting detectors/mode will do (e.g., Olympus Fluoview 1000). The important parameters to set are the laser power, pixel size, and pixel dwell time.

2. For Zeiss in the confocal mode, set up the light path for the PMT detector (see Fig. 12) and for the Leica TCS SP5 (see Fig. 13).

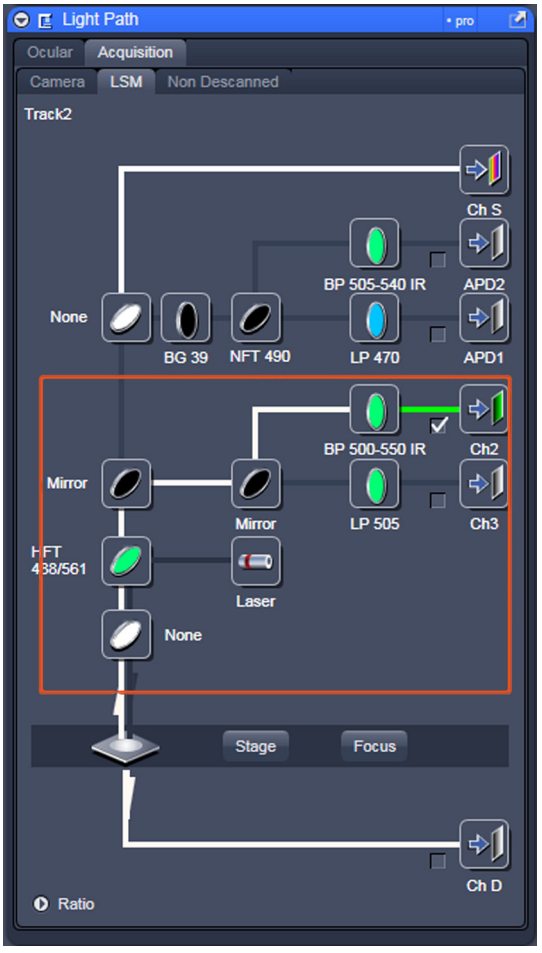

Fig. 12 Light Path window for Zeiss ZEN (version 2008). The dichroic mirror (HFT488/561) and bandpass filter (BP500-550) have been set for EGFP. A check mark indicates Ch2 (PMT) detector is active and the optical path is highlighted in white. An orange box has been added to direct the viewer to the relevant light path parameters. These parameters are used when searching for cells suitable for N&B/RICS acquisition.

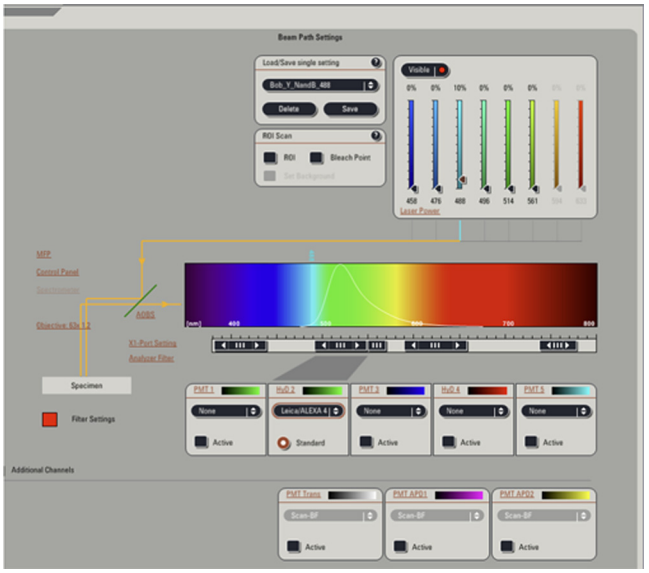

Fig. 13 Light Path and Dyes window for Leica TCS SP5. The filter set for Alexa488 is selected (suitable for EGFP) and the light path is highlighted in yellow. The 488-nm line of the argon laser is set to 10% attenuation and the hybrid detector (HyD2) is set in standard mode. These settings are used when searching for cells suitable for N&B/RICS acquisition.

3. Identify a low-expressing cell [Fig. 14(b)] by opening the pinhole to 3 AU and setting the gain to ~750 or a similar setting depending on the confocal system you are using. Cells with low expression should be barely/moderately visible, which should correspond to a count rate of 20 to 200 kHz when measured for collecting FCS data.

4. Set the acquisition mode settings as shown below and in Fig. 14(a).

   Note: For the Leica microscope systems, the pixel dwell time cannot be set but, instead, the pixel dwell time is determined by the scanner speed (Hz). A scan speed of 100 to 200 Hz is sufficient to acquire RICS and N&B data for most cellular proteins. Settings for Leica TCS SP5 should be as shown in Fig. 15.

   Increase zoom to 17.5 (19.3 for Leica) on a subregion of the chosen cell [Fig. 14(c)]. This zoom is chosen so that the pixel size is equal to 50 nm. This pixel size is important for RICS measurements where the pixel size needs to be three to four times smaller than the radial waist (~200 nm, for 488-nm light) of the confocal volume in order to see the diffusion of the protein molecule.

5. Once the region is selected, change the light path to send emission light to APD and not PMT (Fig. 16).

   For Leica, change to photon counting if a hybrid detector is installed; if not, use APD (Fig. 17).

6. Set APD settings as follows: gain = 1, offset = 0 (if using Leica Hybrid in photon-counting mode, then gain and offset are disabled).

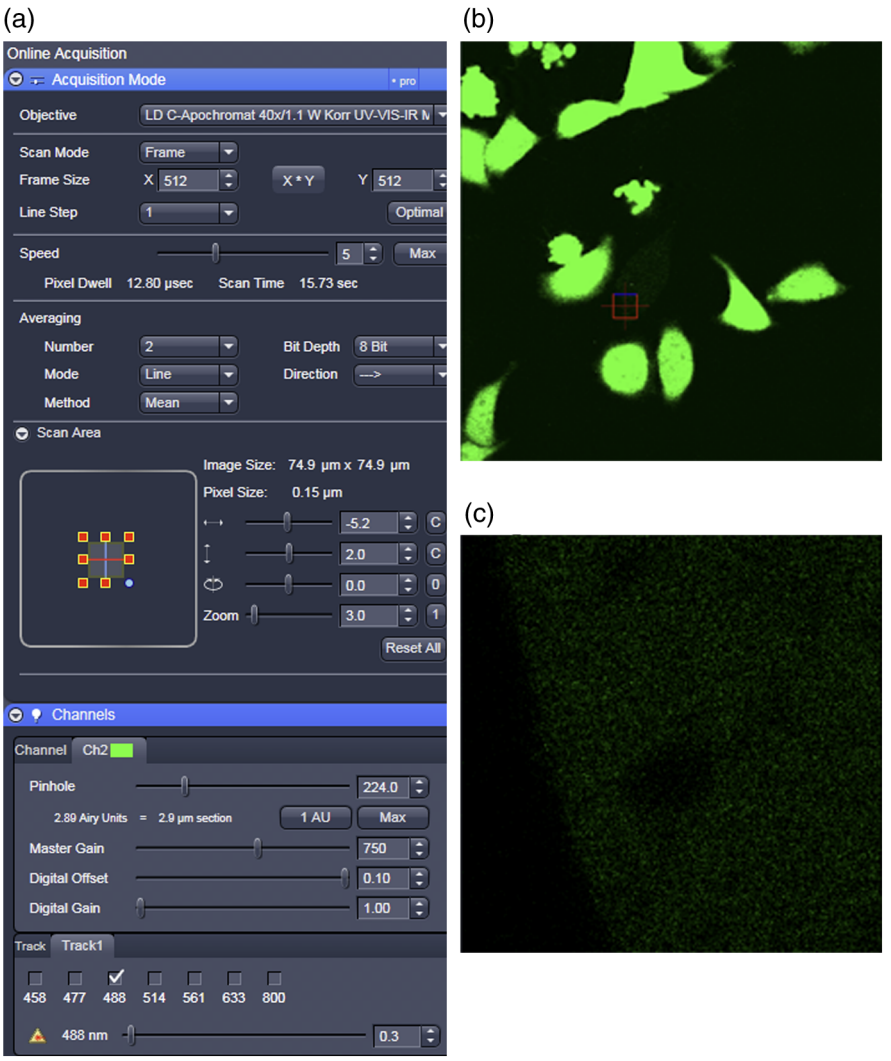

Fig. 14 Acquisition window settings for Zeiss ZEN (version 2008) software for N&B. (a) ZEN acquisition window with the following settings used to collect N&B data: detector set to Ch2 (PMT), scan mode = frame, frame size = 256 × 256, line step = 1, speed = 6 (12.79 μs), line averaging = 1, bit depth = 8, gain = 1, offset = 0, and laser power = 0.3%. (b) Fluorescent image of EGFP expressing HeLa cells—using settings in Fig. 14(a)—with cross-hair on low expressing cell (zoom ~3). (c) High zoom (17.5) of region selected by cross-hair for N&B/RICS acquisition from (b).

Scan mode = frame

Frame size = 256 × 256

Line step = 1

Speed = 6 (12.79 μs per pixel)

Line = 7.656 ms (calculation not shown in Zeiss software)

Frame scan time = 1.96s

Line averaging = 1

Bit depth = 8

Gain = 1, Offset = 0

Laser power = 0.3%

7. >Multidimensional acquisition >Time series: Set interval to zero and acquire 100 images with the above settings. The total acquisition time should take ~3 min.

   For Leica, make sure mode is set to xyt and check box for minimize time interval.

8. Save image series as a Zeiss.lsm file. This image file can be directly analyzed in SimFCS software (Laboratory for Fluorescence Dynamics, UC Irvine) for N&B and RICS. Other confocal microscope system file formats may be supported by SimFCS (see LFD website,[60] but for those not supported, save the file as an 8-bit raw TIFF file. For Leica, export images as raw 8-bit TIFFs.

N&B Analysis Using SimFCS Software

1. Press RICS button on first SimFCS window [Fig. 18(a)].
2. Click on File and then "open multiple images" [Fig. 18(b)].
3. Scroll through the image series to look for any obvious cell movement or artifacts (e.g., vibration distortion, z-drift; Fig. 19). Any images with artifacts should not be

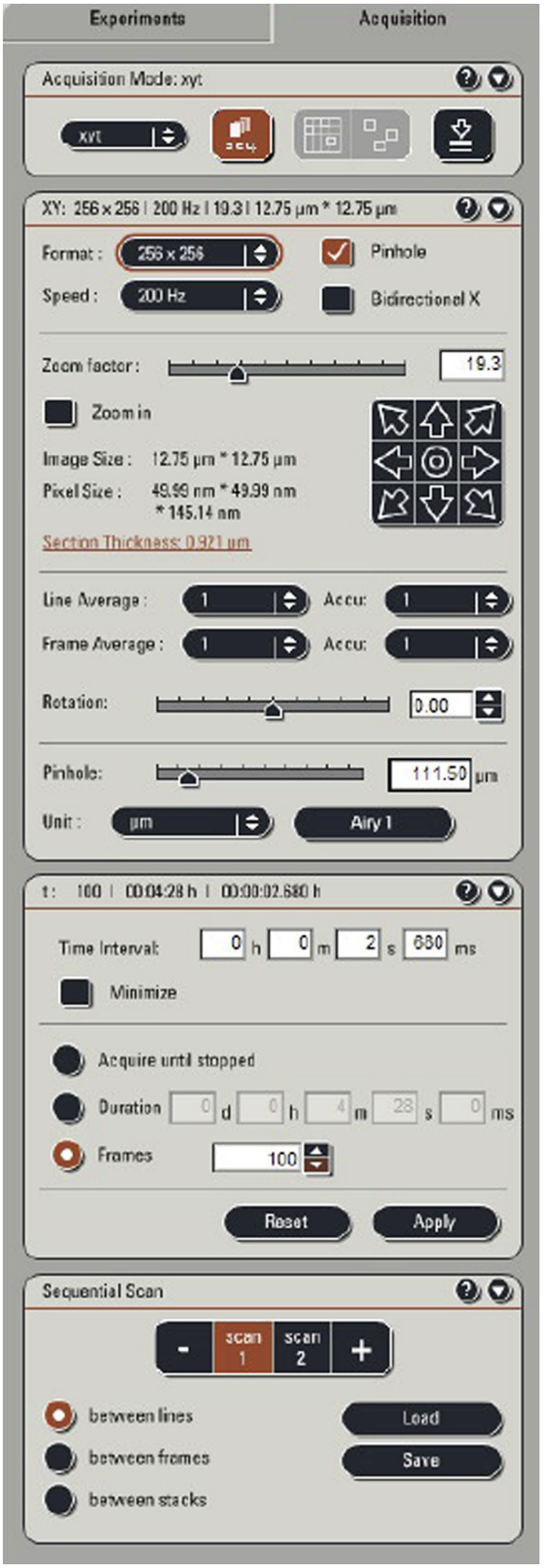

Fig. 15 Acquisition window settings for Leica TCS SP5 software during data acquisition for N&B. Leica acquisition window with the following settings used to collect N&B data: acquisition mode = xyz, frame size = 256×256, line average = 1, frame average = 1 speed = 200 Hz, frames = 100. Make sure to check minimize to remove time delay between frame acquisitions.

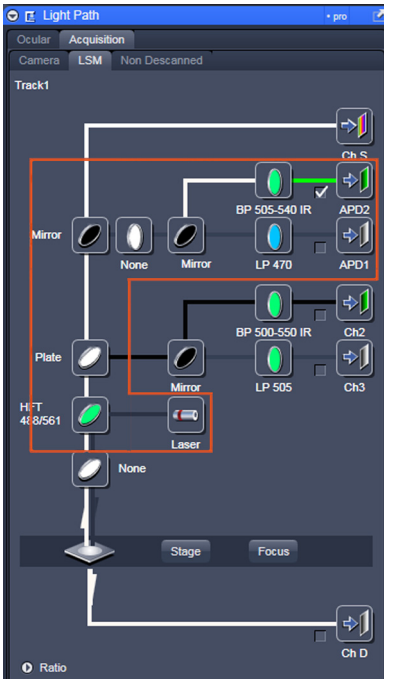

Fig. 16 Light Path window for Zeiss ZEN (version 2008) software for N&B. Same dichroic and bandpass filters as in Fig. 12 are used except that the APD detector is used here. An orange box has been added to direct the viewer to the relevant light path parameters.

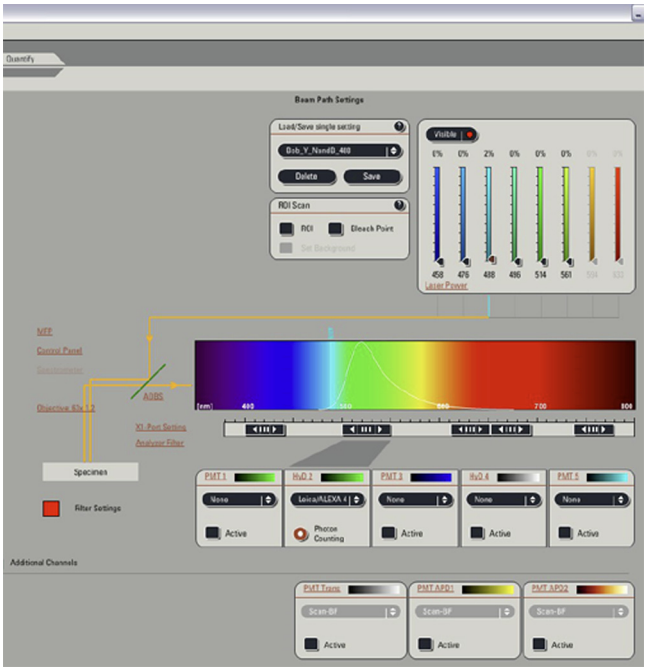

Fig. 17 Light Path window for Leica TCS SP5 software for N&B. Same settings as in Fig. 13 except that the laser is attenuated to 2% and the HyD2 detector is changed from standard to photon-counting mode.

used in the final analysis and can be deleted using the Delete Frame button (Fig. 19). Select the moving average, if needed, and set to 10 as a starting point. The moving average filter removes the slow fluctuations due to cellular movement. Other numbers beside 10 can be

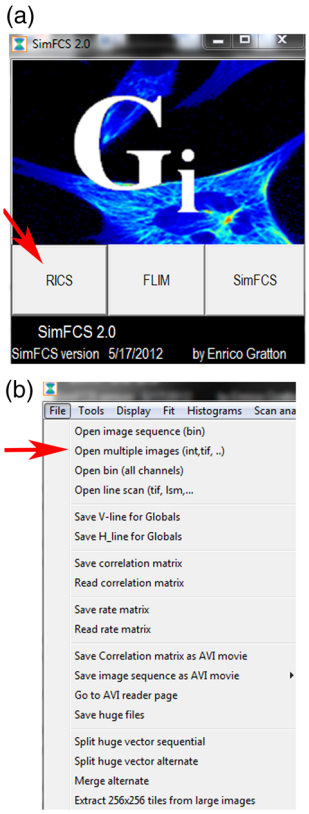

Fig. 18 SimFCS 2.0 Start and File Open windows. (a) Three analysis options (RICS, FLIM, SimFCS) are available upon starting the SimFCS program. The red arrow points to RICS button, which should be selected to start the N&B analysis. (b) Under File select Open Multiple Images (red arrow) to navigate to the folder where your image stack is located. Note: Figures 19 to 27 are all displays/windows in the SimFCS 2.0 software.

tried to match the timescale of the artifact that is to be removed (e.g., 3 or 5).

4. >Tools: Select N&B with option Detrend. If there is no cellular movement, then select No detrend (Fig. 20).
5. A new window (N&B) will open with a B map panel and selection map panel (Fig. 21).
6. Select the Cal tab (Fig. 22), and for our Zeiss system, we enter 0.903 into the *S*_Factor 1 field. The *S* (digital levels) is normally set to 1 for detectors in the photon-counting mode. But in this case, it is adjusted because using the moving average filter causes an artificial lowering of the brightness values (*B*). The *S* value is chosen so that the immobile background outside the cell is equal to 1. The *S* value after detrending can be determined for your system by taking an image series of a thin and uniform fluorescent stationary film. The value needed to adjust the brightness of the film to 1 would be the *S* value needed for correcting after detrending.[21]
7. Press Recalculate N&B button (asterisk in Fig. 22).
8. Under the Filters tab, press the smooth button once to sharpen the brightness map (Fig. 23).
9. Clicking on the Math tab will display the average signal intensity, variance, brightness (true ε), and number of particles (true n, Fig. 24).
10. The pixels of interest can now be highlighted using the cursor on the B map (Fig. 25).

    The red rectangle box highlights the pixels throughout the cytoplasm of the cell that correspond to EGFP.

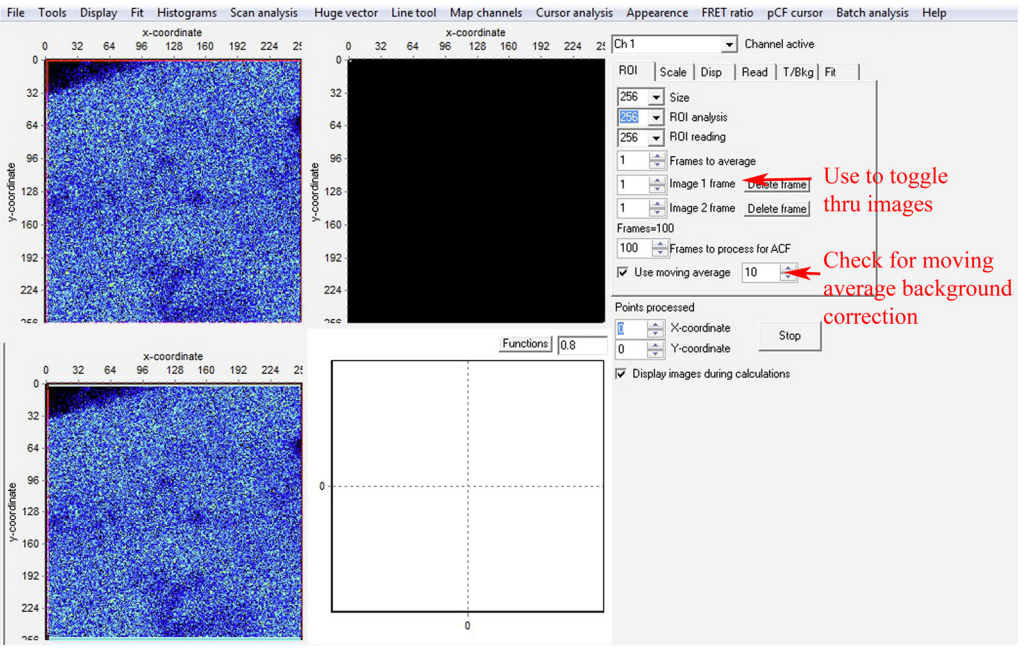

Fig. 19 Main window. In the left image, one of the time series is displayed. To scroll through the stack of images, press the arrow button on image 1 frame (top red arrow). Scroll through the images and delete any images with obvious acquisition artifacts (due to stage drift, cell movement, etc.) (lower red arrow). Make sure to check the Use moving average to filter out slow cellular movement that can cause artifacts.

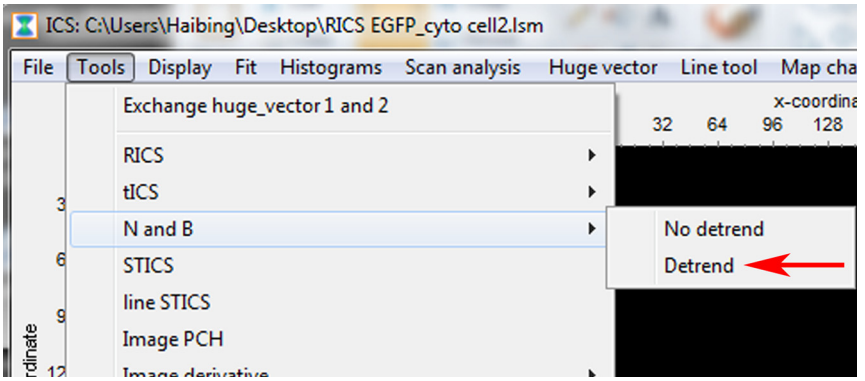

Fig. 20 Tools menu. Select N and B option and Detrend (red arrow) to start the N&B analysis on the image series.

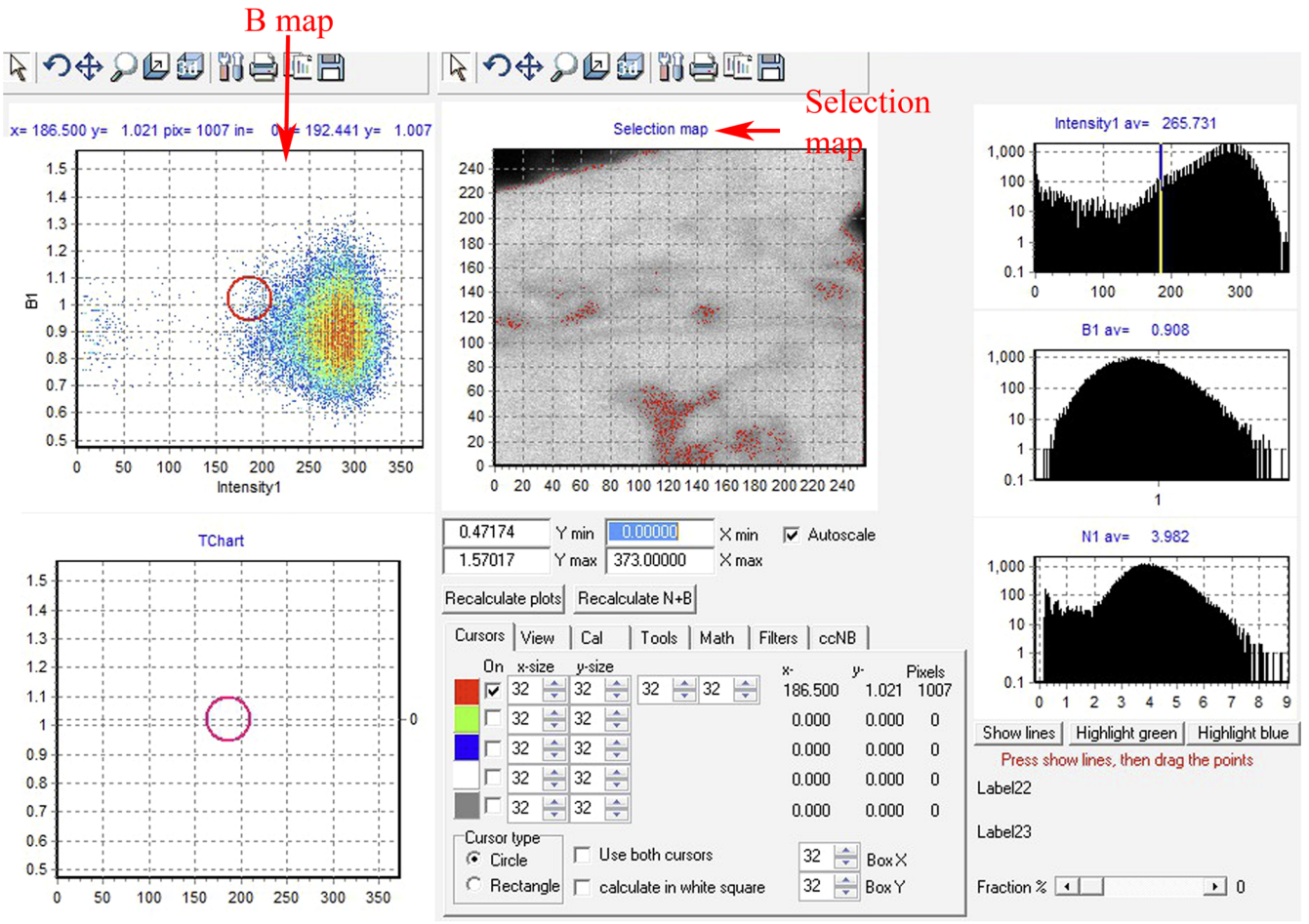

Fig. 21 Analysis window. The upper left panel displays the brightness value ($B1$) as a function of intensity, which we refer to as the B map (red arrow). Next to the B map panel is the selection panel. The far right series of panels displays histograms for average intensity, brightness ($B1$), and number ($N1$). Note: Subtract 1 in order to convert the brightness value to the molecular brightness ($B - 1 = \varepsilon$).

The green rectangle box highlights immobile pixels outside the cell (upper left corner).

The average brightness can be obtained from either above the B map, where $y = 1.051$ (see red arrow in Fig. 25) or from $B1$ average $= 1.042$ (right middle panel). The small difference in values is because of the size and placement of the ROIs selected by the user (y number) versus the program ($B1$ average). Additional ROIs can also be selected for different structures of interest in the cell.

Remember that in the SimFCS program, the B value given is $\varepsilon + 1$, which means the brightness is

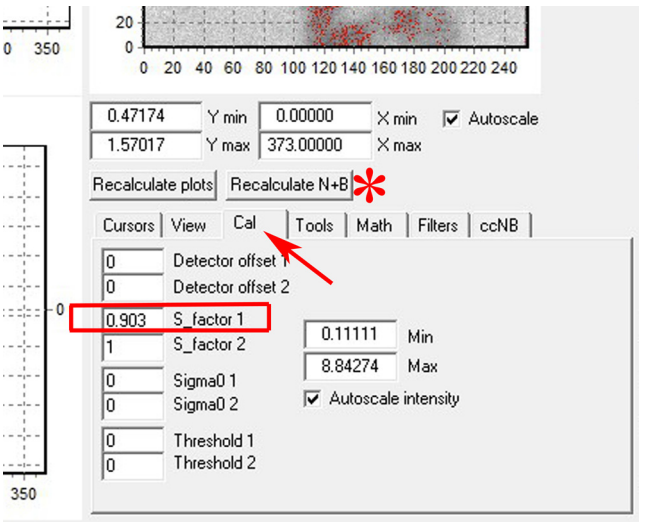

Fig. 22 *B* value correction when employing moving average filter. Select the Cal tab (red arrow) under the selection panel and input the *S* value (red box) and then press the Recalculate N&B button (red asterisk).

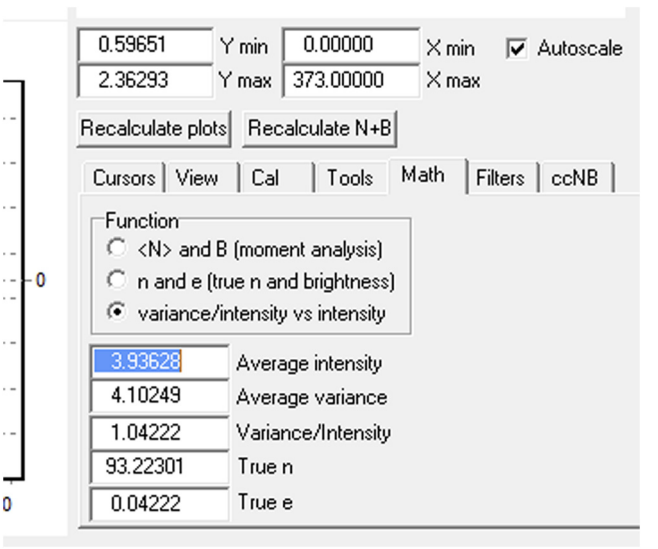

Fig. 24 Math tab in N&B window. Selecting the Math tab displays the average intensity, average variance, variance/intensity, true *e*, and true *n* for the entire image. Regions of interest (ROIs) can be created to calculate the *B* value of that particular region (see Fig. 25).

$1.051 - 1 = 0.051$ cpm. To obtain CPSM, simply divide this number by the pixel dwell time in seconds ($0.051/0.00001279 = 3987$ cpsm). In the math panel, the subtraction of 1 has already been performed, but the conversion to CPSM must be done by the user.

Note: In some cases, there can be an artifact of highly bright pixels along one edge of the field of view (see Fig. 26). This seems to be more prevalent when a subregion of the image is taken for analysis. These are not real particles and represent only a few pixels (80 of 65,461), as can be seen from the frequency versus B plot.

11. Switching back to the original image screen in SimFCS will display the color-coded brightness map and number map.

In Fig. 27, the Scale tab has been selected and the scale for the brightness map has been adjusted by deselecting the automatic feature (red arrow) and setting the range by hand. This allows visual comparison of

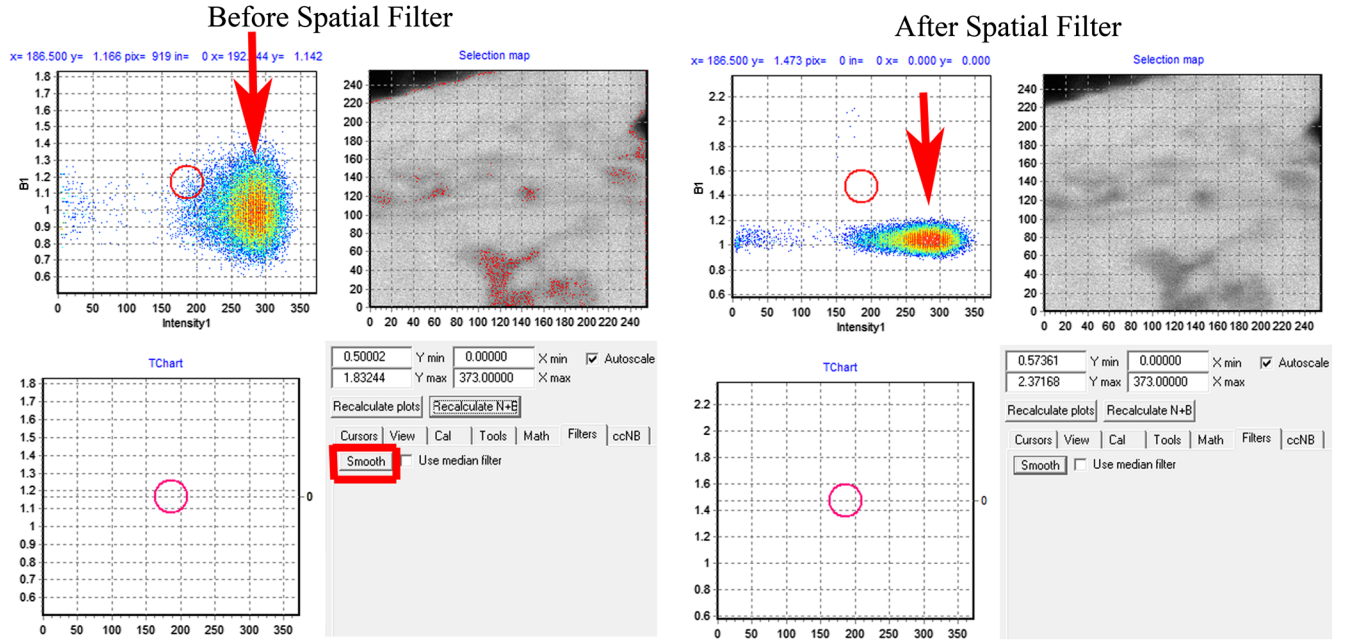

Fig. 23 Use of the spatial filter to sharpen B map. To bin the pixels and sharpen the B map, select the Filters tab and press the Smooth button (red box) once. The smooth filter can be used more than once, but there can be a loss of resolution. For comparison of different samples, it is best to smooth to the same extent.

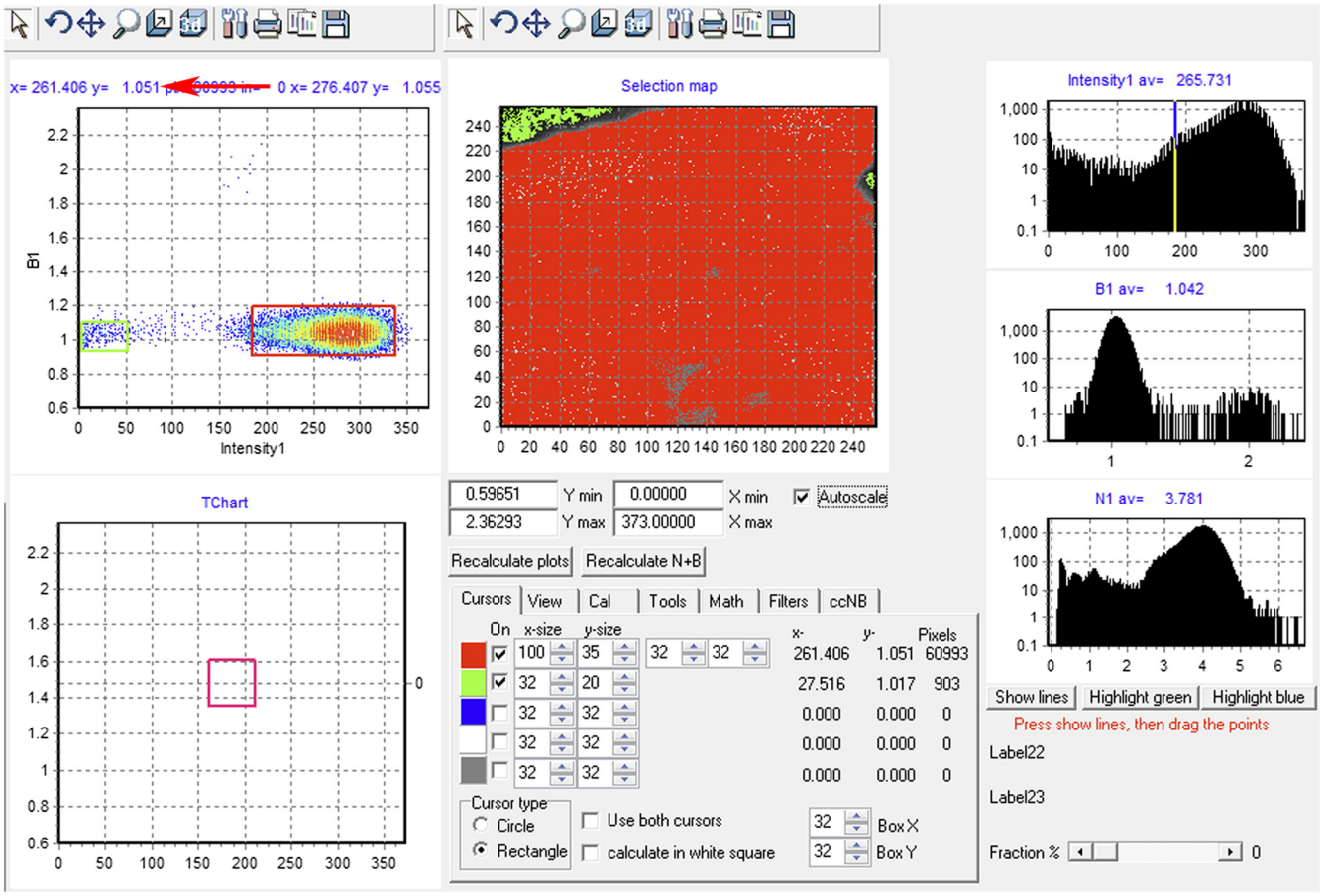

Fig. 25 Selection of ROI in N&B window. Under Cursors tab, select an ROI by clicking on the On box to the left *x* / *y* size. The size of the ROI can be controlled by toggling the *x* or *y* value up and down. The ROI shape can be set as a circle or rectangle. Once the ROI is selected, the box will appear on the B map panel and can be moved around with the mouse cursor. The red arrow points to the location where the B value is displayed for the ROI.

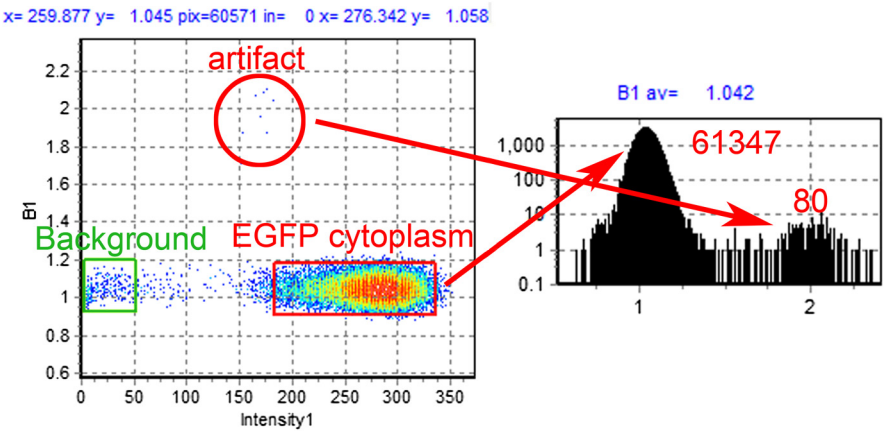

Fig. 26 Representative B map for EGFP in cytoplasm. Left: B map for EGFP expressed in a cell with the pixels corresponding to EGFP in the cytoplasm (red rectangle), background outside the cell (green rectangle), and an artifact (red circle). Right: arrows point to the corresponding pixels in the B value histogram. Note that the number of artificially bright pixels is a fraction (80) of the total pixels (~65,000).

brightness maps between different cells when the scales are set the same. Right clicking on the panels allows for copying to the clipboard or saving the image as a bitmap.

Note: The diffusion of EGFP in the cytoplasm can also be calculated from this image series using the RICS method under the Tools menu. The subtract moving average option should be chosen. The protocol for using SimFCS to calculate average diffusion and for creating diffusion maps will not be discussed here because an excellent protocol for RICS analysis has been written.[61]

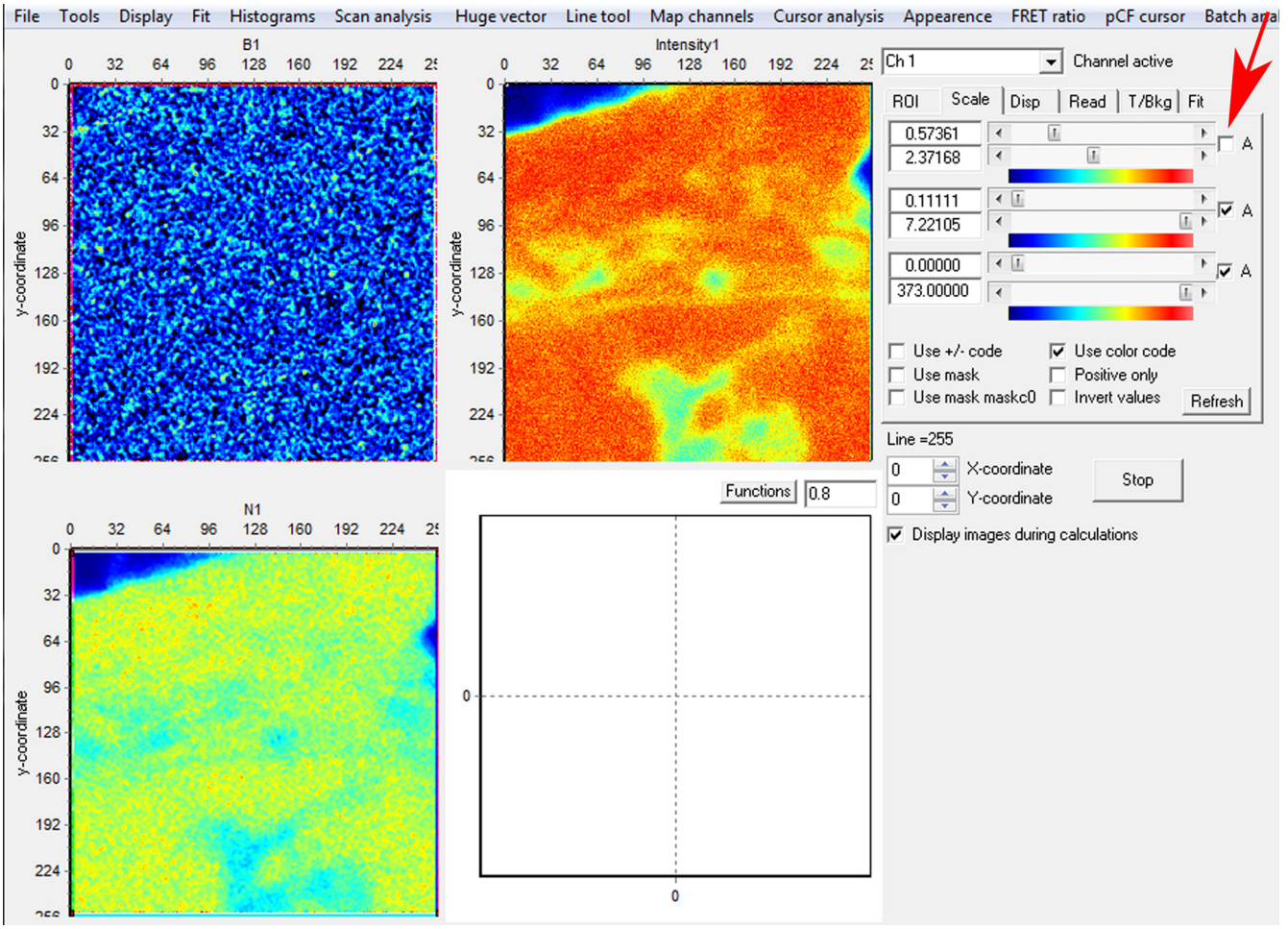

Fig. 27 Main window after N&B analysis. The three panels in the main SimFCS window display color-coded maps for brightness (*B*), number (*N*), and intensity (*I*) after running the N&B calculations. The color palette and ranges (red arrow) for the three parameters can be adjusted under the Scale tab.

Acknowledgments

We thank Michelle Digman for the Paxillin-enhanced green fluorescent protein plasmid and Venkatesan Raghavan for proof-reading and helpful comments. R.T.Y. is grateful for support from the American Heart Association (12SDG8960000) and for imaging support from the Pittsburgh Center for Kidney Research (P30-DK079307). H.T. is supported from the NIH Technology Center for Network and Pathways grant 8U54GM103529 and is grateful for the Shared Imaging Facility at MBIC of Carnegie Mellon University.

References

1. K. Bacia, I. V. Majoul, and P. Schwille, "Probing the endocytic pathway in live cells using dual-color fluorescence cross-correlation analysis," *Biophys. J.* **83**(2), 1184–1193 (2002).
2. E. Adu-Gyamfi et al., "Investigation of Ebola VP40 assembly and oligomerization in live cells using number and brightness analysis," *Biophys. J.* **102**(11), 2517–2525 (2012).
3. K. Bacia et al., "Fluorescence correlation spectroscopy relates rafts in model and native membranes," *Biophys. J.* **87**(2), 1034–1043 (2004).
4. E. Haustein and P. Schwille, "Ultrasensitive investigations of biological systems by fluorescence correlation spectroscopy," *Methods* **29**(2), 153–166 (2003).
5. K. Herrick-Davis et al., "Fluorescence correlation spectroscopy analysis of serotonin, adrenergic, muscarinic, and dopamine receptor dimerization: the oligomer number puzzle," *Mol. Pharmacol.* **84**(4), 630–642 (2013).
6. K. Herrick-Davis et al., "Oligomer size of the serotonin 5-hydroxytryptamine 2C (5-HT2C) receptor revealed by fluorescence correlation spectroscopy with photon counting histogram analysis: evidence for homodimers without monomers or tetramers," *J. Biol. Chem.* **287**(28), 23604–23614 (2012).
7. N. G. James et al., "Number and brightness analysis of LRRK2 oligomerization in live cells," *Biophys. J.* **102**(11), L41–43 (2012).
8. J. D. Muller, Y. Chen, and E. Gratton, "Resolving heterogeneity on the single molecular level with the photon-counting histogram," *Biophys. J.* **78**(1), 474–486 (2000).
9. G. Ossato et al., "A two-step path to inclusion formation of huntingtin peptides revealed by number and brightness analysis," *Biophys. J.* **98**(12), 3078–3085 (2010).
10. P. Schwille et al., "Molecular dynamics in living cells observed by fluorescence correlation spectroscopy with one- and two-photon excitation," *Biophys. J.* **77**(4), 2251–2265 (1999).
11. P. Schwille, J. Korlach, and W. W. Webb, "Fluorescence correlation spectroscopy with single-molecule sensitivity on cell and model membranes," *Cytometry* **36**(3), 176–182 (1999).
12. P. Schwille et al., "Fluorescence correlation spectroscopy reveals fast optical excitation-driven intramolecular dynamics of yellow fluorescent proteins," *Proc. Natl. Acad. Sci. U. S. A.* **97**(1), 151–156 (2000).
13. B. D. Slaughter et al., "SAM domain-based protein oligomerization observed by live-cell fluorescence fluctuation spectroscopy," *PLoS One* **3**(4), e1931 (2008).
14. B. D. Slaughter, J. W. Schwartz, and R. Li, "Mapping dynamic protein interactions in MAP kinase signaling using live-cell fluorescence fluctuation spectroscopy and imaging," *Proc. Natl. Acad. Sci. U. S. A.* **104**(51), 20320–20325 (2007).

15. R. T. Youker et al., "Multiple motifs regulate apical sorting of p75 via a mechanism that involves dimerization and higher-order oligomerization," *Mol. Biol. Cell* **24**(12), 1996–2007 (2013).
16. M. A. Digman et al., "Stoichiometry of molecular complexes at adhesions in living cells," *Proc. Natl. Acad. Sci. U. S. A.* **106**(7), 2170–2175 (2009).
17. J. L. Swift et al., "Quantification of receptor tyrosine kinase transactivation through direct dimerization and surface density measurements in single cells," *Proc. Natl. Acad. Sci. U. S. A.* **108**(17), 7016–7021 (2011).
18. J. Johnson, Y. Chen, and J. D. Mueller, "Characterization of brightness and stoichiometry of bright particles by flow-fluorescence fluctuation spectroscopy," *Biophys. J.* **99**(9), 3084–3092 (2010).
19. J. A. Fitzpatrick and B. F. Lillemeier, "Fluorescence correlation spectroscopy: linking molecular dynamics to biological function in vitro and in situ," *Curr. Opin. Struct. Biol.* **21**(5), 650–660 (2011).
20. B. D. Slaughter and R. Li, "Toward quantitative 'in vivo biochemistry' with fluorescence fluctuation spectroscopy," *Mol. Biol. Cell.* **21**(24), 4306–4311 (2010).
21. M. A. Digman, M. Stakic, and E. Gratton, "Raster image correlation spectroscopy and number and brightness analysis," *Methods Enzymol.* **518**, 121–144 (2013).
22. D. Magde, E. L. Elson, and W. W. Webb, "Fluorescence correlation spectroscopy. II. An experimental realization," *Biopolymers* **13**(1), 29–61 (1974).
23. E. L. Elson and W. W. Webb, "Concentration correlation spectroscopy: a new biophysical probe based on occupation number fluctuations," *Annu. Rev. Biophys. Bioeng.* **4**(1), 311–334 (1975).
24. U. Meseth et al., "Resolution of fluorescence correlation measurements," *Biophys. J.* **76**(3), 1619–1631 (1999).
25. Y. Chen et al., "The photon counting histogram in fluorescence fluctuation spectroscopy," *Biophys. J.* **77**(1), 553–567 (1999).
26. Y. Chen et al., "Molecular brightness characterization of EGFP in vivo by fluorescence fluctuation spectroscopy," *Biophys. J.* **82**(1 Pt 1), 133–144 (2002).
27. M. A. Digman et al., "Mapping the number of molecules and brightness in the laser scanning microscope," *Biophys. J.* **94**(6), 2320–2332 (2008).
28. M. A. Digman et al., "Measuring fast dynamics in solutions and cells with a laser scanning microscope," *Biophys. J.* **89**(2), 1317–1327 (2005).
29. P. Macdonald et al., "Brightness analysis," *Methods Enzymol.* **518**, 71–98 (2013).
30. N. Dross et al., "Mapping eGFP oligomer mobility in living cell nuclei," *PLoS One* **4**(4), e5041 (2009).
31. S. T. Hess and W. W. Webb, "Focal volume optics and experimental artifacts in confocal fluorescence correlation spectroscopy," *Biophys. J.* **83**(4), 2300–2317 (2002).
32. D. A. Bulseco and D. E. Wolf, "Fluorescence correlation spectroscopy: molecular complexing in solution and in living cells," *Methods Cell Biol.* **72**, 465–498 (2003).
33. S. A. Kim, K. G. Heinze, and P. Schwille, "Fluorescence correlation spectroscopy in living cells," *Nat. Methods* **4**(11), 963–973 (2007).
34. E. Haustein and P. Schwille, "Fluorescence correlation spectroscopy: novel variations of an established technique," *Annu. Rev. Biophys. Biomol. Struct.* **36**, 151–169 (2007).
35. R. E. Rigler, Ed., *Fluorescence Correlation Spectroscopy: Theory and Applications*, Springer, New York (2001).
36. J. Ries and P. Schwille, "Fluorescence correlation spectroscopy," *Bioessays* **34**(5), 361–368 (2012).
37. H. Qian and E. L. Elson, "Distribution of molecular aggregation by analysis of fluctuation moments," *Proc. Natl. Acad. Sci. U. S. A.* **87**(14), 5479–5483 (1990).
38. H. Qian and E. L. Elson, "On the analysis of high order moments of fluorescence fluctuations," *Biophys. J.* **57**(2), 375–380 (1990).
39. Y. Chen, L. N. Wei, and J. D. Muller, "Probing protein oligomerization in living cells with fluorescence fluctuation spectroscopy," *Proc. Natl. Acad. Sci. U. S. A.* **100**(26), 15492–15497 (2003).
40. A. G. Palmer, III and N. L. Thompson, "High-order fluorescence fluctuation analysis of model protein clusters," *Proc. Natl. Acad. Sci. U. S. A.* **86**(16), 6148–6152 (1989).
41. A. G. Palmer, III and N. L. Thompson, "Fluorescence correlation spectroscopy for detecting submicroscopic clusters of fluorescent molecules in membranes," *Chem. Phys. Lipids* **50**(3–4), 253–270 (1989).
42. N. L. Thompson, *Fluorescence Correlation Spectroscopy*, Plenum Press, New York (1991).
43. C. M. Brown et al., "Raster image correlation spectroscopy (RICS) for measuring fast protein dynamics and concentrations with a commercial laser scanning confocal microscope," *J. Microsc.* **229**(01), 78–91 (2008).
44. P. Kask et al., "Fluorescence-intensity distribution analysis and its application in biomolecular detection technology," *Proc. Natl. Acad. Sci. U. S. A.* **96**(24), 13756–13761 (1999).
45. T. D. Perroud, B. Huang, and R. N. Zare, "Effect of bin time on the photon counting histogram for one-photon excitation," *Chemphyschem* **6**(5), 905–912 (2005).
46. J. D. Muller, "Cumulant analysis in fluorescence fluctuation spectroscopy," *Biophys. J.* **86**(6), 3981–3992 (2004).
47. K. Palo et al., "Fluorescence intensity multiple distributions analysis: concurrent determination of diffusion times and molecular brightness," *Biophys. J.* **79**(6), 2858–2866 (2000).
48. R. B. Dalal et al., "Determination of particle number and brightness using a laser scanning confocal microscope operating in the analog mode," *Microsc. Res. Tech.* **71**(1), 69–81 (2008).
49. L. Gelman and J. Rietdorf, "Routine assessment of fluorescence microscope performance," 2010, http://www.imaging-git.com/science/light-microscopy/routine-assessment-fluorescence-microscope-performance.
50. V. Buschmann et al., "Quantitative FCS: Determination of the Confocal Volume by FCS and Bead Scanning with the MicroTime 200 (application note, PicoQuant)," http://www.picoquant.com/scientific/technical-and-application-notes/category/technical_notes_techniques_and_methods (22 September 2014).
51. R. Swaminathan, C. P. Hoang, and A. S. Verkman, "Photobleaching recovery and anisotropy decay of green fluorescent protein GFP-S65T in solution and cells: cytoplasmic viscosity probed by green fluorescent protein translational and rotational diffusion," *Biophys. J.* **72**(4), 1900–1907 (1997).
52. A. Labilloy et al., "Altered dynamics of a lipid raft associated protein in a kidney model of Fabry disease," *Mol. Genet. Metab.* **111**(2), 184–192 (2014).
53. M. A. Digman et al., "Paxillin dynamics measured during adhesion assembly and disassembly by correlation spectroscopy," *Biophys. J.* **94**(7), 2819–2831 (2008).
54. N. Altan-Bonnet and G. Altan-Bonnet, "Fluorescence correlation spectroscopy in living cells: a practical approach," *Curr. Protoc. Cell Biol. 4.24*, 1–14 (2009).
55. T. J. Stasevich et al., "Cross-validating FRAP and FCS to quantify the impact of photobleaching on in vivo binding estimates," *Biophys. J.* **99**(9), 3093–3101 (2010).
56. A. Trullo et al., "Application limits and data correction in number of molecules and brightness analysis," *Microsc. Res. Tech.* **76**(11), 1135–1146 (2013).
57. J. Unruh, "Stowers ImageJ Plugins," http://research.stowers.org/imagejplugins/zipped_plugins.html (22 September 2014).
58. L. N. Hillesheim and J. D. Muller, "The dual-color photon counting histogram with non-ideal photodetectors," *Biophys. J.* **89**(5), 3491–3507 (2005).
59. L. N. Hillesheim and J. D. Muller, "The photon counting histogram in fluorescence fluctuation spectroscopy with non-ideal photodetectors," *Biophys. J.* **85**(3), 1948–1958 (2003).
60. Enrico Gratton, "Tutorials for Globals Software," http://www.lfd.uci.edu/globals/tutorials/ (22 September 2014).
61. M. J. Rossow et al., "Raster image correlation spectroscopy in live cells," *Nat. Protoc.* **5**(11), 1761–1774 (2010).

Robert T. Youker is an assistant professor of molecular biology at Western Carolina University in North Carolina. He received his PhD in molecular, cellular, and developmental biology from the University of Pittsburgh and then performed postdoctoral studies at the Vollum Institute and the University of Pittsburgh. He uses cell biology, biochemistry, and biophysical imaging approaches to study diverse cellular processes, including protein sorting and degradation.

Haibing Teng has been a microscopy core facility manager for 14 years. She is trained in medicine and biology/neuroscience (PhD from University of Missouri and postdoctoral in Indiana University and Washington University). She has extensive experience in light and electron microscopy preparations and quantitative image analysis approaches.